Serum Proteomic Signature of Human Chagasic Patients for the Identification of Novel Potential Protein Biomarkers of Disease*[S]

Jian-Jun Wen‡, M. Paola Zago§, Sonia Nuñez¶, Shivali Gupta‡, Federico Nuñez Burgos¶, and Nisha Jain Garg‡‖**

Chagas disease is initiated upon infection by *Trypanosoma cruzi*. Among the health consequences is a decline in heart function, and the pathophysiological mechanisms underlying this manifestation are not well understood. To explore the possible mechanisms, we employed IgY LC10 affinity chromatography in conjunction with ProteomeLab PF2D and two-dimensional gel electrophoresis to resolve the proteome signature of high and low abundance serum proteins in chagasic patients. MALDI-TOF MS/MS analysis yielded 80 and 14 differentially expressed proteins associated with cardiomyopathy of chagasic and other etiologies, respectively. The extent of oxidative stress-induced carbonyl modifications of the differentially expressed proteins (n = 26) was increased and coupled with a depression of antioxidant proteins. Functional annotation of the top networks developed by ingenuity pathway analysis of proteome database identified dysregulation of inflammation/acute phase response signaling and lipid metabolism relevant to production of prostaglandins and arachidonic acid in chagasic patients. Overlay of the major networks identified prothrombin and plasminogen at a nodal position with connectivity to proteome signature indicative of heart disease (*i.e.*, thrombosis, angiogenesis, vasodilatation of blood vessels or the aorta, and increased permeability of blood vessel and endothelial tubes), and inflammatory responses (*e.g.*, platelet aggregation, complement activation, and phagocyte activation and migration). The detection of cardiac proteins (myosin light chain 2 and myosin heavy chain 11) and increased levels of vinculin and plasminogen provided a comprehensive set of biomarkers of cardiac muscle injury and development of clinical Chagas disease in human patients. These results provide an impetus for biomarker validation in large cohorts of clinically characterized chagasic patients. ***Molecular & Cellular Proteomics 11: 10.1074/mcp.M112.017640, 435–452, 2012.***

From the ‡Department of Microbiology and Immunology, the ‖Faculty of the Institute for Human Infections and Immunity, Center for Tropical Diseases, and the Sealy Center for Vaccine Development, University of Texas Medical Branch, Galveston, Texas 77555-1070, the §Instituto de Patología Experimental, Consejo Nacional de Investigaciones Científicas y Técnicas-Universidad Nacional de Salta, Salta CP: 4400, Argentina, and the ¶Servicio de Cardiología, Hospital San Bernardo, Salta CP: 4400, Argentina

Received February 2, 2012, and in revised form, April 17, 2012
Published, MCP Papers in Press, April 27, 2012, DOI 10.1074/mcp.M112.017640

Chagas disease continues to present a serious threat to human health in Latin America and is one of the most important emerging parasitic diseases in developed countries including the United States (1). According to a World Health Organization report released in 2010, an estimated 10 million people are infected, and >25 million people are at risk of infection in endemic countries (2). It is assessed that >300,000 infected patients live in the United States (3). Up to 40% of chronically infected individuals develop cardiac alterations, and up to 10% develop digestive, neurological or mixed alterations, resulting in considerable morbidity and mortality (4).

Human plasma and serum are the most easily available, clinically valuable specimens. Besides abundant proteins, *e.g.*, albumin, immunoglobulin, transferrin, haptoglobin, and lipoprotein, plasma and serum contain many other proteins that are secreted or released from cells and tissues throughout the body. In chronic conditions or disease states, as is also noted in chagasic patients (5, 6), modification of the proteome manifests as a result of disease-associated changes in specific genes up- or down-regulation, isoform switching, or *de novo* protein synthesis (7, 8). Further, progression of disease severity, presented by an increasing order of cardiac injury and cell death (9, 10), may also result in the release of intracellular proteins in the peripheral system, thus altering the proteome profile. It is thus logical to assume that the pathological processes during the development of Chagas disease would cause characteristic changes in the circulating proteins and generate a detectable, disease-specific molecular phenotype.

In addition to changes in proteome profile, post-translational protein modifications in response to disease-associated stress also contribute to protein change resulting from modification of specific amino acids. We have documented in experimental animal models and human chagasic patients

that reactive oxygen species (ROS)[1] of inflammatory and mitochondrial origin contribute to oxidative modification of proteins in peripheral blood and myocardium (11–14). For example, treatment of infected animals with an antioxidant was effective in arresting oxidative cardiac pathology (15) and preventing the loss of cardiac left ventricular function in chronic hearts (16), thus establishing the pathological significance of oxidative overload in Chagas disease. To date, however, proteomic examples of oxidative modification identification in cardiovascular diseases are lacking.

The plasma/serum proteome is the most useful version of the human proteome for clinical investigations and patient diagnostic and treatment purposes. Nevertheless, clinical proteomics, *i.e.*, translation of proteomic techniques to study clinical pathology, has not been widely used. The two-dimensional polyacrylamide gel electrophoresis (2D-GE) method enables identification of major proteins in a tissue or subcellular fraction by mass spectrometric methods and can be used to compare quantities of proteins in related samples (17). However, 2D-GE has many drawbacks, including a narrow dynamic range that requires the multistep removal of abundant proteins before low abundance serum proteins or biomarkers can be detected, problematic solubilization and separation of hydrophobic proteins, and a restricted ability to load limited sample amounts on a gel (~250 μg) (18). Poor reproducibility of gel images between experiments, imprecise quantitation, and intensive labor requirements are additional limitations in applying the 2D-GE approach for clinical proteome analysis (19).

The ProteomeLab™ PF2D system offers an alternative approach to protein profiling that addresses issues of complexity and utilization of fractions after analysis. PF2D is designed to allow automated separation of proteins in the first dimension by pI-based chromatofocusing, followed by a second dimension hydrophobicity-based separation of proteins by reverse phase (RP)-HPLC (20). Changing the composition or pH range of elution buffer allows increased resolution of hydrophobic, basic, or acidic proteins, a process that cannot be achieved by 2D-GE (21). Importantly, all protein fractions from PF2D are collected in 96-well plates from which they can be easily lyophilized and submitted for mass spectrometric protein/peptide identification or utilized for immunoblotting, catalytic staining, or other assays. The in-built scanning spectrophotometer allows one to simultaneously monitor the normal and oxidatively modified isoforms of the proteins in second dimension fractions for the automated, efficient detection of disease-associated protein oxidative and other (*e.g.*, phosphorylation) modifications (22).

In this study, we investigated the host physiological and pathological changes at the protein level in chagasic human patients. We employed IgY-12 chemistry to separate the serum-abundant proteins and the PF2D system to develop the protein signature of low abundance serum proteins in Chagas disease patient samples. We also made use of traditional one- and two-dimensional gel electrophoresis and ELISA to identify serum-abundant proteins that were differentially expressed or oxidized in chagasic patients. Our findings of a number of proteins that were differentially expressed in patients provide clues to the pathomechanisms that contribute to Chagas disease.

MATERIALS AND METHODS

Human Subjects—Human sera samples from chagasic and non-chagasic/other cardiomyopathy patients used in this study were obtained from Salta, Argentina and Chiapas, Mexico. Sera samples from seronegative healthy individuals exhibiting no history or clinical symptoms of cardiac disease from the same geographical area were used as controls. All of the procedures were approved by the institutional review boards at the University of Texas Medical Branch, Universidad Nacional de Salta, Argentina, and the Universidad Autónoma de Chiapas, Mexico.

In Argentina, written informed consent was obtained from all individuals (age range: 19–71 years, 56% females) before their enrollment in the study. Venous blood samples were collected without anticoagulant to obtain serum. *Trypanosoma cruzi*-specific antibodies in sera samples were monitored by an enzyme-linked immunosorbent assay using a Wiener Chagatest-ELISA recombinant v.4.0 kit comprising six recombinant proteins known to be expressed in mammalian stage of *T. cruzi* in isolates circulating in Latin America. Briefly, 96-well plates were coated with recombinant proteins and then sequentially incubated with 20-μl sera samples (1:20 dilution) and horseradish peroxidase-conjugated human monoclonal anti-IgG and color-developed with chromogenic substrate monitored by spectrometry at 450 nm (cutoff value: average of seronegative samples ($<$0.1 optical density) + 0.2 optical density, *i.e.*, $\geq$0.3). Serological tests were also done following the specifications of the commercial Indirect Heamagglutination test kit (Wiener Chagatest-HAI). Briefly, sera samples (25-μl 4-fold dilutions) were mixed with red blood cells sensitized with *T. cruzi* cytoplasmic and membrane antigens and agglutination-monitored. The titer was defined as the highest serum dilution presenting agglutination (positive $\geq$ 1:16 dilution). Those positive by both tests were identified as seropositive. The clinical data included medical history, physical examination, subjective complaint of frequency and severity of exertional dyspnea, 12-lead electrocardiography at rest to obtain a comprehensive view of cardiac rhythm and conduction abnormalities, 3-lead electrocardiography with exercise to note major cardiac rhythm alterations, transthoracic echocardiogram to obtain objective information regarding the left ventricular contractile function, and chest x-ray to assess cardiomegaly (cardiothoracic ratio $>$ 0.5). The severity of exertional dyspnea was graded according to the New York Heart Association classification (23). Based on these criteria, seropositive chagasic patients exhibiting no echocardiographic abnormalities, preserved systolic function (ejection fraction $\geq$ 55%), and no left ventricular dilatations, but with negligible to minor electrocardiography alterations were graded as clinically asymptomatic. Seropositive patients were graded clinically symptomatic if they exhibited varying degrees of systolic dysfunction

[1] The abbreviations used are: ROS, reactive oxygen species; 2D-GE, two-dimensional gel electrophoresis; CC, cardiomyopathy of chagasic origin; CO, cardiomyopathy of other etiologies; DNPH, 2,4-dinitrophenylhydrazine; IPA, Ingenuity pathways analysis; IPG, immobilized pH gradient; MYH11, myosin heavy chain 11; MYL2, myosin light chain 2; NN, normal subjects with no disease; PLG, plasminogen; RP, reverse phase; VCL, vinculin; VIM, vimentin; WB, Western blotting.

(ejection fraction 40–54% or less) and/or left ventricular dilatation (end diastolic diameter ≥ 57 mm). Seronegative cardiomyopathy patients of other etiologies (CO) were categorized by criteria similar to those of the chagasic patients. Seronegative, healthy controls were recruited from the same geographical area.

In Mexico, human sera samples (age range: 18–73 years, 55% females) were collected within the framework of a research project on emerging zoonotic diseases conducted jointly by several institutions, including Chiapas State University, Mexican Social Security Institute, Chiapas Health Institute, and University of Texas Medical Branch at Galveston. All of the samples were screened by ELISA, flow cytometry, and Stat-Pak (Chembio Diagnostic Systems, Medford, NY) to distinguish seropositive and seronegative samples before inclusion in the study (24). The seropositive subjects generally represented the indeterminate/asymptomatic form of the disease.

Separation of High Abundance Sera Proteins—To enrich the low abundance proteins for enhanced detection, we employed the IgY-12 high capacity LC10 proteome partitioning system (Beckman Coulter, Brea, CA) in combination with the ProteomeLab PF2D system (Beckman), according to the manufacturer's instructions (details in supplemental File 1). The collected low abundance proteins in the flow through fractions consisted of 4.8–10% of the proteins present in the original whole serum, and 90–95.2% of the total proteins were captured as major (abundant) proteins by IgY columns. To obtain sufficient quantities of low abundance proteins for PF2D analysis, we processed five aliquots (total 1250 μl) of each sera sample by IgY-12 chromatography. The flow through (enriched low abundance proteins) and eluted (high abundance proteins) serum fractions were neutralized, concentrated by using Amicon® ultracentrifugal filters (3-kDa cutoff; Millipore), and desalted by PD-10 desalting columns (GE Healthcare). Protein content was determined by using the Bradford assay (Bio-Rad).

Protein Profiling by ProteomeLab PF2D System—Serum protein fractionation using PF2D system was carried out by high performance chromatofocusing in the first dimension and RP-HPLC in the second dimension. Briefly, after equilibration, the samples (2.5 mg of protein in 100 μl) were injected onto the chromatofocusing column, and first dimension fractionation was performed using a pH gradient 8.3–3.5, the fractions being collected with the fraction collector/injector module at 0.3-pH intervals. For the second dimension separation, selected first dimension fractions (250 μl) were injected into the RP-HPLC column and run for 2 min with solvent A (0.1% trifluoroacetic acid in HPLC water). The column was then eluted with a linear gradient of 0–100% solvent B (0.08% trifluoroacetic acid in acetonitrile) for 33 min, and second dimension fractions were collected at 30-s intervals in 96-well plates.

ProteoVue software (Eprogen) was utilized to convert chromatographic intensities of fractions collected after a second dimension RP-HPLC fractionation of each of the first dimension fractions collected in pH gradient 8.3–4.0. This analysis produced a highly detailed heat map of each sample, incorporating the dimensions of pI (*x* axis) and hydrophobicity (*y* axis). DeltaVue software was employed to compare derived intensity bands from ProteoVue analysis of any two samples, allowing quantitative differences in protein contents measured by peak area (volume). Finally, Karat 32 software was employed to compare significantly different peaks among multiple samples and to identify proteins. Detailed methods for protein profiling by PF2D and comparative proteome analysis are presented in supplemental File 1.

Profiling of High Abundance Serum Proteins by Two-dimensional Gel Electrophoresis—We rehydrated 11-cm immobilized pH gradient (IPG) strips (pH 3–10, pH 4–7, or pH 7–10 [from Bio-Rad]) at 50 V for 12 h in 250 μl of rehydration buffer (1 M thiourea, 8 M urea, 2% CHAPS, 1% dithiothreitol, and 0.2% ampholytes (Bio-Rad)) containing 200 μg of protein sample ($n = 4$/sample) and 0.002% of bromphenol blue. Isoelectric focusing was performed at 500 V for 1 h, 1000 V for 1 h, 8000 V for 2 h, and then 8000 V for a total of 50,000 Vh (25). The IPG strips were suspended in equilibration buffer (50 mM Tris-HCl, pH 6.8, 6 M urea, 20% glycerol) and sequentially incubated for 15 min each in the presence of 2% DTT, 2% SDS (reducing conditions) and 2.5% iodoacetamide, 2% SDS (alkylating conditions). Equilibrated IPG strips were subjected to second dimension electrophoresis by using 8–10% linear gradient precast Tris-HCl gels (Bio-Rad) on a PROTEAN plus Dodeca cell system at 75 V for 1 h and then at 120 V until the dye front reached the bottom of the gel. The gels were fixed in 10% methanol, 7% acetic acid, stained with SYPRO Ruby (Bio-Rad), destained in 10% ethanol, 7% acetic acid, and imaged by using a high resolution ProXPRESS proteomic imaging system (PerkinElmer Life Sciences).

In total, 12 Sypro Ruby-stained two-dimensional gels ($n = 18$/group) were digitalized on a ProXPRESS proteomic imaging system (PerkinElmer Life Sciences), and the images were analyzed on Progenesis SameSpotst™ software 2.0 (NonLinear Dynamics). Normalized spot volumes, *i.e.*, the volume of each spot over the volume of all spots in the gel, were used for comparison of the different groups, and candidates were identified as protein spots that changed in expression level by >2-fold as compared with normal controls. Statistical significance was assessed by the analysis of variance test, and p values of <0.05 were considered significant for comparison (26).

Detection of Carbonyl Proteins—We employed Western blotting (WB) in conjunction with one- or two-dimensional gel electrophoresis to detect the carbonyl modifications in low abundance and high abundance protein sera fractions, respectively (27, 28) (supplemental File 1).

Mass Spectrometry and Protein Identification—Please see supplemental File 1 for detailed methods for processing of fractionated protein samples collected after second dimension PF2D analysis and protein containing gel spots from two-dimensional gels. Peptide mixtures (1 μl) obtained after tryptic digestion were directly spotted onto a MALDI-TOF MS/MS target plate with 1 μl of α-cyano-4-hydroxycinnamic acid matrix solution (5 mg/ml in 50% acetonitrile). Peptides were analyzed by using a MALDI-TOF/TOF™ ABI 4800 proteomics analyzer (Applied Biosystems). The Applied Biosystems software package included the 4000 Series Explorer (v. 3.6 RC1) with Oracle Database Schema Version (v. 3.19.0) and Data Version (3.80.0) to acquire and analyze MS and MS/MS spectral data. The instrument was operated in a positive ion reflectron mode with the focus mass set at 1700 Da (mass range, 850–3000 Da). For MS data, 1000–2000 laser shots were acquired and averaged from each protein spot. Automatic external calibration was performed by using a peptide mixture with the reference masses 904.468, 1296.685, 1570.677, and 2465.199. Following MALDI MS analysis, MALDI MS/MS was performed on several (5–10) abundant ions from each protein spot. A 1-kV positive ion MS/MS method was used to acquire data under post-source decay conditions. The instrument precursor selection window was ± 3 Da. Automatic external calibration was performed by using reference fragment masses 175.120, 480.257, 684.347, 1056.475, and 1441.635 (from precursor mass 1570.700).

Applied Biosystems GPS Explorer™ (v. 3.6) software was employed in conjunction with MASCOT (v.2.2.07) to search the NCBI human protein database (last accessed January 25, 2011; 17,148,519 entries) by using both MS and MS/MS spectral data for protein identification. Protein match probabilities were determined by using expectation values and/or MASCOT protein scores. The MS peak filtering included the following parameters: a mass range of 800–3000 Da, minimum Signal-to-Noise filter = 10, mass exclusion list tolerance = 0.5 Da, and mass exclusion list for some trypsin and keratin-containing compounds included masses of 842.51, 870.45, 1045.56,

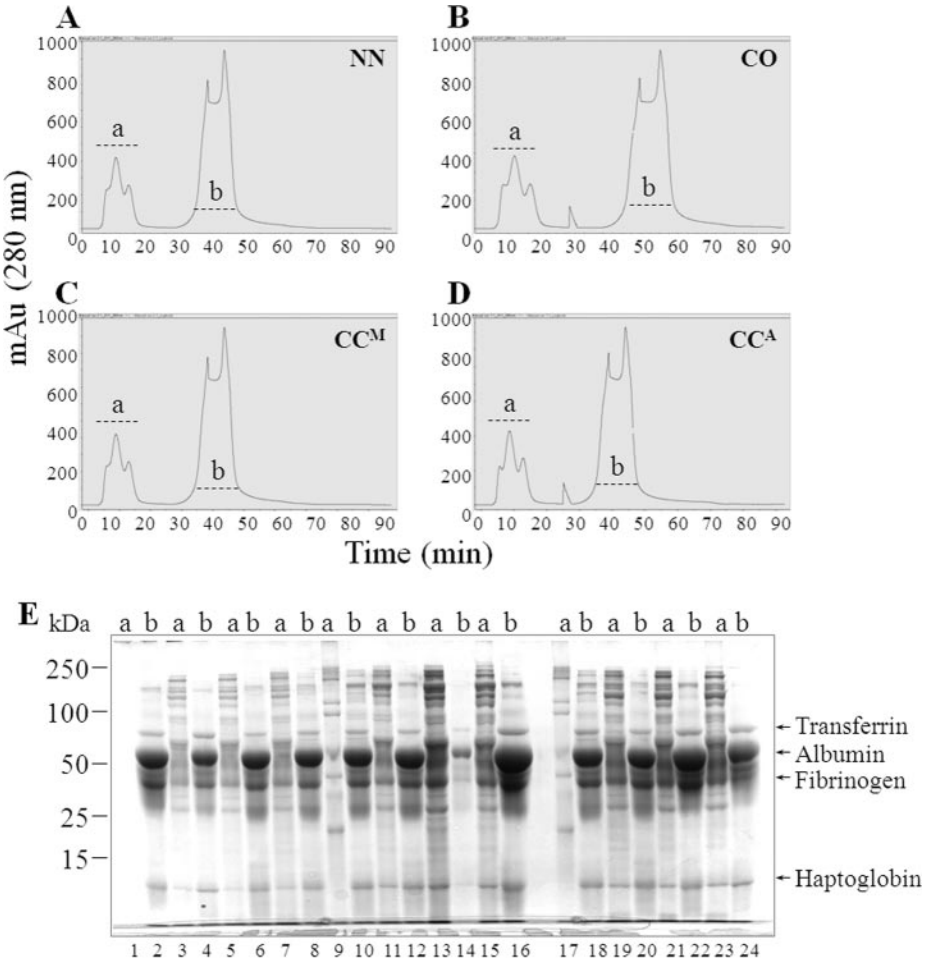

FIG. 1. **Immunodepletion of human sera samples.** *A–D*, human sera (250 μl) samples were partitioned by using ProteomeLab IgY-12 column chromatography at an absorbance of 280 nm to remove the 12 high abundance proteins. The enriched pool of low abundance proteins (*fraction a*, 5–22 min) and the high abundance proteins bound to the column (*fraction b*, 30–50 min) were collected for further analysis. *E*, shown is SDS-PAGE analysis of *fractions a* and *b* collected from sera samples of normal subjects with no disease (NN, *lanes 1–6*), patients with cardiomyopathy of other etiologies (CO, *lanes 7–12*), and seropositive chagasic subjects from Mexico (CC^M, *lanes 13–18*) and Argentina (CC^A, *lanes 19–24*).

1179.60, 1277.71, 1475.79, and 2211.1 Da. The MS/MS peak filtering included the following parameters: minimum S/N filter = 10, maximum missed cleavages = 1, fixed modification of carbamidomethyl, variable modifications caused by oxidation, precursor tolerance = 0.2 Da, MS/MS fragment tolerance = 0.3 Da, mass = monoisotopic, and peptide charges = +1. The significance of a protein match, based on the peptide mass fingerprint in the MS and the MS/MS data from several precursor ions, is presented as expectation values ($p < 0.001$). To confirm the identified proteins were of human and not of parasite origin, we also performed a similar search against NCBI nonredundant protein database consisting of *T. cruzi* sequences.

Functional Analysis—All data sets were assessed by using an online tool (http://www.uniprot.org/uniprot, UniProt release February 8, 2011) to predict the Gene Ontology and recognize the function of the identified proteins. Ingenuity pathways analysis (IPA, Ingenuity Systems®) was performed to integrate the identified proteins into networks and signaling pathways with biological meaning and significance. IPA was also employed to rapidly gain biological insight and access a comprehensive overview of scientific findings including biological functions, molecular interactions, regulatory events, and pharmacological relevance. An e-value was calculated by estimating the probability of a random set of proteins having a frequency of annotation for that term greater than the frequency obtained in the real set, and a threshold of 10^{-3} was set to retrieve significant molecular functions and biological processes. With these parameters, we were able to highlight the most informative and significantly over-represented Gene Ontology terms in the data set (29).

Sera Screening for Detection of Disease Biomarkers—The 96-well microtiter plates were coated overnight at 4 °C with 100-μl sera samples in 0.1 M carbonate buffer, pH 9.6 (1:50, v/v), and blocked for 2 h at room temperature with 1% nonfat dry milk. The plates were then sequentially incubated with 100 μl each of antibodies against MYL2, VCL, and VIM (Santa Cruz, 1:3000) for 2 h, horseradish peroxidase-labeled IgG antibody (Southern Biotech, 1:5000) for 1 h, and Sure blue TMB substrate for 15 min. The reaction was blocked with 2 N sulfuric acid and colorimetric change in absorbance was measured at 450 nm on a SpectraMax 190 microplate reader (Molecular Devices). The ELISA results were normalized to total protein concentration, determined by Bio-Rad protein assay. Plasminogen levels were measured using a sandwich ELISA kit from ICL Inc.

RESULTS

Immunodepletion of High Abundance Proteins in Serum—Compared with other sample types such as bronchial lavage, cerebrospinal fluid, and tears, plasma/serum consist of a wide dynamic range of protein concentration, and the high abundance proteins interfere with the detection of low abundance potential biomarker proteins (30, 31). To enhance our ability to detect low abundance proteins, we employed IgY-12 LC10 immunoaffinity columns and performed HPLC to separate high abundance proteins. Shown in Fig. 1 (*A–D*) are repre-

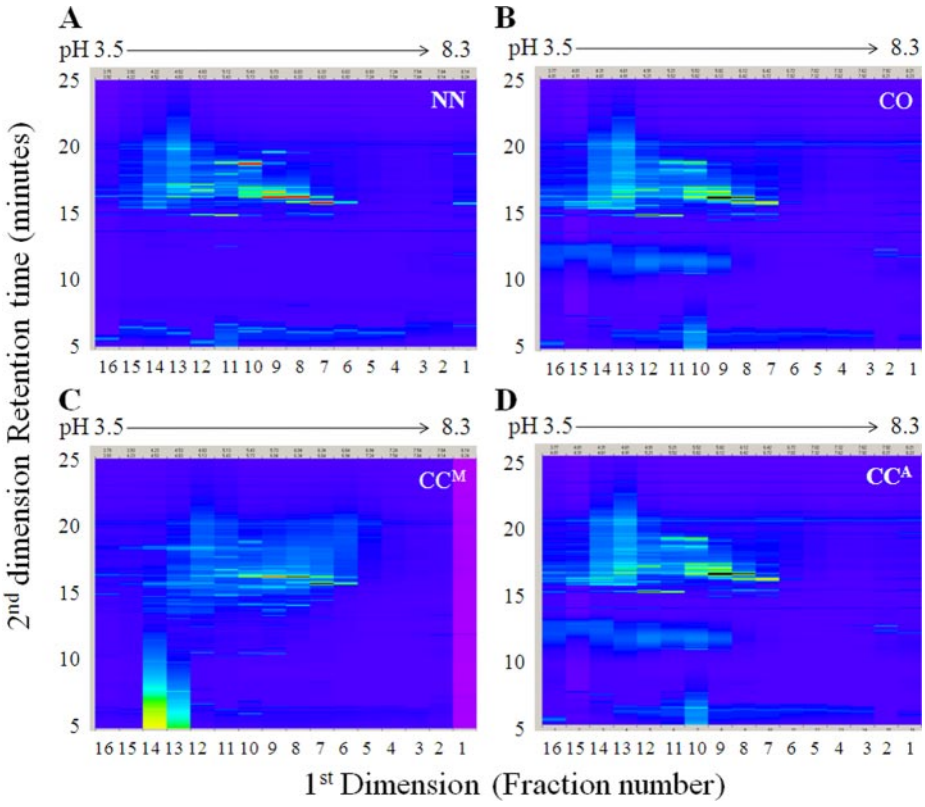

FIG. 2. **PF2D two-dimensional heat maps.** Sera samples, enriched in low abundance proteins, were subjected to PF2D analysis. PF2D first dimension separation is based on pI, and second dimension separation utilizes reverse phase-HPLC. Shown are PF2D ProteoVue heat maps of representative serum samples from normal subjects with no disease (NN) (*A*), patients exhibiting cardiomyopathy of other etiologies (CO) (*B*), and seropositive, chagasic subjects from Mexico (CC^M) (*C*) and Argentina (CC^A) (*D*). ProteoVue displays the *pI* for first dimension fractions on the *x* axis and the second dimension retention time as the *y* axis. The color scheme ranges from *purple* (low absorbance) to *red* (high absorbance) and indicates the protein band intensity, measured at 214 nm.

sentative IgY-12 LC10 affinity chromatographs of sera samples from normal subjects with no disease (NN), seronegative individuals exhibiting cardiomyopathy of other etiologies (CO), seropositive (clinically asymptomatic) subjects from Mexico (CC^M), and chagasic (clinically symptomatic) patients from Argentina (CC^A). The distinct separation of flow through fractions (5–25 min, marked *a*) enriched in low abundance proteins and column-bound high abundance proteins (eluted during 30–50 min, marked *b*) indicate that serum low abundance proteins were effectively depleted of high abundance proteins by IgY-12 LC10 column chromatography. Polyacrylamide gel analysis (Fig. 1*E*) confirmed the above results and showed the abundant proteins, *e.g.*, transferrin, albumin, fibrinogen, and haptoglobin, were separated in the bound fraction and not detectable in the low abundance protein fraction for all sera samples.

PF2D/Mass Spectrometric Analysis of Serum Proteomic Signature of Low Abundance Proteins in Chagasic Patients—We examined the reproducibility of the PF2D system by submitting enriched sera samples from normal healthy subjects to first dimension high performance chromatofocusing on different days (supplemental Fig. S1*A*) and then submitted triplicates of first dimension fractions for second dimension RP-HPLC analysis (supplemental Fig. S1*B*). We observed high reproducibility of retention time for both first and second dimension fractions collected for the same and diverse sera samples on different days and obtained precise alignment of peaks among replicate runs. These data showed that it is feasible to resolve complicated protein mixtures with high reproducibility by using the ProteomeLab PF2D system.

For identifying disease-specific serum profiles, we injected 2.5 mg of each enriched sera sample into the first dimension column. In general, for normal subjects as well as patient groups, we recovered 30% of proteins in the 8.3–3.5 pH gradient, 31% before the initiation of the pH gradient (pH>8.0), and the remaining 39% eluted when the column was finally washed with high salinity buffer (supplemental Fig. S2). We concentrated on 16 fractions collected in the pH 8.3–3.5 range gradient, which were subjected to a second dimension by using RP-HPLC. Representative virtual two-dimensional gel images of sera proteome of normal, chagasic, and other cardiomyopathy subjects, combining the first and the second dimension and viewing proteins separated by pI and hydrophobicity, are shown in Fig. 2. By using the paired peak function in DeltaVue mapping tools, we aligned and analyzed the second dimension chromatograms for each first dimension fraction of two groups for quantitative and qualitative analysis (supplemental Fig. S3*A*). A composite MultiVue comparison of peaks during the second dimension fractionation of first dimension fractions (supplemental Fig. S3*B*) clearly indicated that the shift in retention time for any particular peak among the four groups was less than 10 s and confirmed that we could provide reliable comparative analysis of the second dimension peaks from different samples based upon retention time.

DeltaVue is limited in the simultaneous analysis of more than two samples. We therefore utilized the functions of Karat

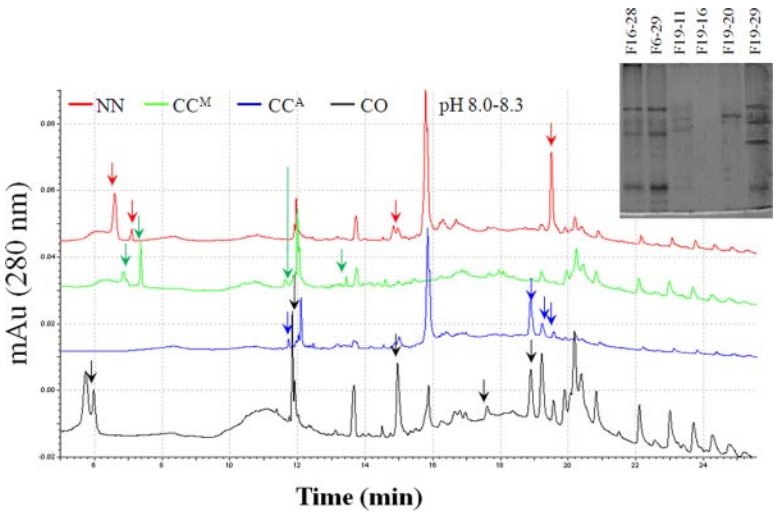

FIG. 3. **Comparative analysis of ProteomeLab second dimension fractionation of low abundance sera proteins from chagasic and other cardiomyopathy subjects.** Sera samples enriched in low abundance proteins from normal subjects (NN, *red*), patients exhibiting cardiomyopathy of other etiologies (CO, *black*), and seropositive chagasic (CC) individuals from Argentina (CC^A, *blue*) and Mexico (CCM, *green*) were subjected to first dimension pH gradient (pH 8.3–3.5), and fractions were collected at 0.3-pH intervals. The first dimension fractions were then subjected to second dimension RP-HPLC. Shown are the representative second dimension protein UV traces (214 nm) of the first dimension fraction collected at pH 8.0–8.3. For clarity, the UV traces were staggered by 0.005 mAu (absorbance unit). Comparative second dimension protein UV traces (214 nm) of the first dimension fractions collected at pH 0.3 intervals during pH 8.0–3.5 gradient are shown in supplemental Fig. S4. *Inset*, fourth dimension resolution of PF2D second dimension fractions from a seropositive/chagasic subject on an 8% reducing polyacrylamide gel, stained with Coomassie Brilliant Blue G-250.

32 software to generate and overlay second dimension protein UV traces of multiple samples. Representative second dimension protein UV traces (214 nm) of the first dimension fractions collected at pH 0.3 intervals during the pH 8.0–8.3 gradient for normal, chagasic, and other cardiomyopathy patient samples are shown in Fig. 3 and supplemental Fig. S4. The comparative analysis of second dimension UV traces of first dimension fractions collected at a pH gradient of $>$8.0, $<$4.0 and between 4–8.3 showed that a majority of peaks were generated from first dimension fractions collected at the pH 4–8.3 gradient, and there was no statistically significant difference in the number of total peaks (range: 1285–1688) generated for samples from different groups (supplemental Fig. S5, *A–D*). Of these, the percentage of matching protein peaks among different groups was $>$85%, demonstrating an extensive homology in the protein profile of cardiomyopathy patients of chagasic or other etiologies with that of normal subjects. The differentially expressed protein peaks detected in normal controls, seropositive subjects from Mexico, chagasic patients from Argentina, and other cardiomyopathy patients from Argentina, marked with color-coded arrows in Fig. 3 and supplemental Fig. S4, were 27 $\pm$ 1.3, 76 $\pm$ 6.1, 82 $\pm$ 4.5, and 57 $\pm$ 5, respectively. These data indicated that (*a*) some sera proteins, *i.e.*, those that were differentially expressed in normal subjects, were depressed in chagasic patients' sera, and (*b*) chagasic patients exhibited a higher rate of differentially expressed proteins than noted in patients with cardiomyopathy of other etiologies.

Toward discovery of proteins that are of potential significance in characterizing the disease state and severity, our next task was the identification of differentially expressed protein peaks by mass spectrometry. For this, selected second dimension fractions were either directly subjected to MALDI-TOF MS analysis or further resolved on 8% acrylamide gels to visualize the differences in the polypeptide composition, and gel slices containing differentially expressed protein bands were submitted for MALDI-TOF MS identification. The *inset* in Fig. 3 shows a typical SDS-PAGE analysis of a second dimension fraction from chagasic patients. The protein peaks for sequencing were chosen based upon their maximal differential expression ($\geq$2-fold) in seropositive, chagasic groups as compared with normal subjects. The MS and MS/MS spectral data were submitted to the UniProt human proteome database for identification of proteins, and then homology searches were conducted against NCBI and SwissProt databases to validate protein identity. These analyses yielded 108 protein identifications with high probability, some of which were identified more than once. Overall, we identified 16, 13, and 64 low abundance proteins that were overexpressed in normal subjects (*i.e.*, decreased in chagasic subjects), other cardiomyopathy patients, and chagasic patients, respectively (Table I).

2D-GE/Mass Spectrometric Analysis of Serum Proteomic Signature of High Abundance Proteins in Chagasic Patients—The high abundance serum proteins, eluted from the IgY-12 columns, were resolved by 2D-GE to obtain a disease-specific abundant protein signature. In initial analysis, when using

TABLE I

Proteome profile of low abundance protein sera fractions in human patients with cardiomyopathy of chagasic and other etiologies

Human sera samples were depleted of high abundance proteins using IgY-12 high capacity LC10 proteome partitioning chromatography. The enriched, low abundance proteins were resolved by the ProteomeLab PF-2D approach, and protein fractions eluted after second dimension high performance reverse phase chromatography were collected in 96-well plates. Proteins fractions/protein peaks uniquely detected in sera samples from normal healthy subjects with no disease, cardiomyopathy patients of other etiologies and chagasic patients were subjected to MALDI-TOF MS/MS analysis, and proteins identified by homology search against Swiss-prot database. The putative biological function and cellular location were identified using ingenuity pathway analysis and the UniProt system. The selected, differentially expressed protein fractions were resolved by SDS-PAGE and subjected to Western blotting with anti-DNPH antibody to detect DNPH-derivatized carbonyl post-translational modification. The extent of carbonylation is recorded as − (absent) or +, ++, and +++ when <25%, 25–50%, and >50% of the expressed protein was modified. NA, information not available in public databases.

Gene name	Protein name	Swiss-Prot GI number	Protein molecular mass (kDa)	Protein score (%)	Protein pI	Carbonylation	Biological/molecular function	Cellular location
Protein peaks specific to normal subjects with no disease (*i.e.*, down-regulated in chagasic subjects)								
APOC3	Apolipoprotein C-III	114026	10,846	100	5.23	−	Lipid transport	Extracellular
ATG16L1	Autophagy protein 16-L1	62510482	68,223	90.83	6.2	−	Protein transport	Cytoplasm
C4BPA	C4b-binding protein α	416733	66,989	100	7.15	−	Innate response	Extracellular
CLPB	Caseinolytic peptidase B	25009267	78,680	94.96	9.13	−	Heat response	NA
CLU	Clusterin	116533	52,461	100	5.89	−	Anti-apoptotic	Extracellular
DPP10	Dipeptidyl peptidase 10	57628	90,876	81.70	6.11	−	Proteolysis	Membrane
EEA1	Early endosome antigen 1	229462866	162,367	88.72	5.55	−	Endosomal	Membrane
F2	Prothrombin	135807	69,992	100	5.64	−	Acute phase response	Extracellular
IGHA1	Immunoglobulin heavy α-1	113584	37,631	100	6.08	−	Immune response	Extracellular
IGHA2	Immunoglobulin heavy α-2	218512088	36,503	100	5.71	−	Immune response	Membrane
KIAA1210	Uncharacterized protein	262527575	186,905	89.94	8.72	−	NA	NA
KRT2	Keratin, type II cytoskeletal 2	239938650	65,393	93.36	8.07	−	Epidermis develop	Intermediate filament
MYH14	Myosin heavy chain 14	71151982	227,863	97.17	5.76	−	Cell shape	Myosin complex
PRL	Prolactin	130930	25,859	78.99	6.5	−	Cell proliferation	Extracellular
SPATA1	Spermatogenesis-associated protein 1	205830058	50,276	92.01	8.54	−	NA	NA
TTR	Transthyretin	136464	15,877	87.04	5.52	−	Transport	Extracellular
Protein peaks specific to patients with cardiomyopathy of other etiologies								
AMBP	α-1-Microglobulin	122801	38,974	71	5.95	−	Host-pathogen	Extracellular
C4B	Complement C4-B	81175167	192,673	286	6.73	−	Inflammatory	Extracellular
CKAP2L	Cytoskeleton assoc protein 2	224471891	83,466	83.69	9.82	−	NA	NA
COL21A1	Collagen type XXI α-1	74752071	99,307	88.45	8.57	−	Cell adhesion	Cytoplasm
GPLD1	Glycan-sp phospholipase D	126302583	92,278	180	5.91	−	Protein release	Secreted
HIST1H2B	Histone cluster 1H2B type 1	462236	13,942	158	10.31	−	Nucleosome assembly	Nucleus
ITIH2	Inter-α trypsin inhibitor H2	229462889	106,397	511	6.4	−	Hyaluronan metabolism	Extracellular
KNG1	Kininogen 1	124056474	71,912	104	6.34	−	Vasodilation	Extracellular
PCID2	PCI domain-protein 2	85681034	46,000	79.47	8.78	−	NA	NA
SERPING1	Serpin peptidase inhibitor G1	124096	55,119	171	6.09	−	Innate immune response	Extracellular
SUCLG2	Succinyl-CoA ligase 2	52788292	46,481	60.87	6.15	−	Carbohydrate metabolism	Mitochondria
TTLL8	Tubulin tyrosine ligase-like 8	190410987	90,698	97.90	8.48	−	Protein polyglycylation	Cytoplasm
VCL	Vinculin	21903479	123,722	79.5	5.5	−	Muscle contraction	Extracellular
Protein peaks specific to patients with cardiomyopathy of chagasic origin								
BCL2A1	Bcl-2-related protein A1	2493280	20,119	64.31	5.33	+++	Anti-apoptotic	Cytoplasm
C14ORF57	Uncharacterized protein	71152045	14,664	86.74	9.34	−	NA	NA
C4BPA	C4b-binding protein α	416733	66,989	100	7.15	+++	Innate immune response	Extracellular
C9orf135	Uncharacterized protein	74746987	26,428	87.63	6.75	−	NA	Membrane
CASP10	Caspase-10	12644463	58,913	89.22	6.95	+++	Apoptosis	NA
CFB	Complement factor B	584908	85,479	99.95	6.67	−	Complement activation	Extracellular
CP	Ceruloplasmin	116117	122,128	100	5.44	−	Oxidation reduction	Extracellular
CTTN	Cortactin	168693629	61,549	59.03	5.24	−	NA	Cytoplasm

TABLE I—*continued*

Gene name	Protein name	Swiss-Prot GI number	Protein molecular mass (kDa)	Protein score (%)	Protein pI	Carbonylation	Biological/molecular function	Cellular location
DAPL1	Death-associated protein-like 1	167012060	11,873	75.87	10	−	Apoptosis	NA
DCPS	Scavenger mRNA-decapper	116241325	38,585	83.69	5.93	−	mRNA catabolism	Nucleus
DIP2A	Disco-interacting protein 2A	32700084	170,261	76.42	8.35	−	Catalytic activity	Nucleus
DNAH17	Dynein heavy chain 17	172044714	511,460	94.72	5.56	−	Microtubule movement	Cytoplasm
F13B	Coagulation factor XIII B	145559473	75,461	99.25	6.01	−	Blood coagulation	Extracellular
CCNB1	G2/mitotic-specific cyclin-B1	116176	48,306	72.93	7.09	−	Cell cycle	Spindle pole
GC	Vitamin D-binding protein	139641	52,929	100	5.4		Transport	Extracellular
GCNT1	Glucosaminyl (*N*-acetyl) transferase 1	218512053	49,767	65.92	8.65	−	Protein modification	Integral to membrane
GFAP	Glial fibrillary acidic protein	121135	49,850	62.63	5.42	−	NA	Cytoplasm
GMDS	GDP-mannose 4,6 dehydratase	9087147	41,923	94.21	6.87	+++	Leukocyte adhesion	Cytoplasm
GNPDA1	Glucosamine-6-phosphate deaminase 1	1171639	32,648	97.42	6.32	+++	Carbohydrate metabolism	Cytoplasm
H1FOO	Histone H1oo protein	74762503	35,792	98.21	4.22–4.52	−	Meiosis	Cytoplasm
HNRNPM	Heterogeneous nuclear ribonucleoprotein M	55977747	77,464	98.58	8.84	−	mRNA splicing	Nucleus
HRG	Histidine-rich glycoprotein	123523	59,541	100	7.09	−	Blood coagulation	Extracellular
KIAA1370	Uncharacterized protein	166218826	121,594	95.19	8.12	−	NA	NA
KLC2	Kinesin light chain 2	13878553	68,892	66.70	6.72	++	Transport	Cytoplasm
KRT1	Keratin, type II cytoskeletal 1	238054406	65,999	100	8.15	++, +++	Oxidative response	Membrane
KRT2	Keratin, type II cytoskeletal 2	239938650	65,393	82.92	8.07	+++	Keratinization	Intermediate
KRT6A	Keratin, type II 6A	1346344	60,008	99.89	8.09	+, +++	Cell differentiation	Keratin filament
KRT6B	Keratin, type II 6B	238054404	60,030	99.02	8.09	+	Cell differentiation	Intermediate
KRT6C	Keratin, type II 6C	59803089	59,988	98.79	8.09	+	Cell differentiation	Intermediate
KRT9	Keratin, type I cytoskeletal 9	239938886	62,027	100.00	5.14	− to +++	Intermediate filament organization	Intermediate
KRT10	Keratin, type I cytoskeletal 10	269849769	58,792	98.04	5.13	−, +++	Cell proliferation	Intermediate
KRT14	Keratin, type I cytoskeletal 14	229463044	51,529	99.77	5.09	+	Cell proliferation	Intermediate
KRT15	Keratin, type I cytoskeletal 15	216548460	49,167	77.48	4.71	−	Epidermis development	Intermediate
KRT16	Keratin, type I cytoskeletal 16	23503075	51,236	87.63	4.99	−, +	Epidermis development	Intermediate
KRT25	Keratin, type I cytoskeletal 25	74723316	49,287	78.50	5	−	Epidermis development	Intermediate
MED14	Mediator complex subunit 14	145559461	160,504	87.63	8.97	−	Transcription regulation	Nucleus
MSH2	MutS protein homolog 2	1171032	104,677	92.01	5.58	−	DNA repair	Nucleus
MYO1C	Myosin-1c	226694178	121,648	71.65	9.48	+++	Transport	Membrane
MEF2C	Myocyte-specific enhancer factor 2C	2500875	51,189	72.30	8.14	−	Transcription regulation	Nucleus
MYL2	Myosin light chain 2	149067749	17,670	89.33	4.96	−	Immune response	Cytoplasm
MYH11	Myosin heavy chain 11	13432177	227,199	93.04	5.42	−	Cardiac muscle	Myosin
NDEL1	Nuclear distribution nudE-1	74725006	38,352	61.76	4.22–4.52	−	Transport	Cytoplasm
NRAP	Nebulin-related anchoring protein	115502505	196,950	79.93	9.24	−	Ribosomal biogenesis	Nucleus
NUMA1	Nuclear mitotic apparatus protein 1	145559510	238,115	95.90	5.63	− to +++	Nucleus organization	Cytoplasm
OSBPL8	Oxysterol-binding protein 8	39932732	101,132	95.40	7.24–7.54	+++	Transport	NA
PCID2	PCI domain-containing protein 2	85681034	46,000	99.99	8.78	−	NA	NA
PCNT	Pericentrin	188595720	377,850	93.65	5.39	−	Cytoskeletal	Cytoplasm
PDE4A	Phosphodiesterase 4A	116242706	98,081	70.99	5.09	−	Signal transduction	Membrane
PHB2	Prohibitin-2	74752151	33,276	100	3.92–4.22	+++	Transcription	Cytoplasm
PLG	Plasminogen	130316	90,510	63.48	7.04	−	Tissue remodeling	Extracellular
RNF115	RING finger protein 115	56405389	33,682	65.13	5.39	+++	Ubl conjugation	Cytoplasm
RTEL1	Regulator of telomere elongation helicase 1	229462743	133,599	72.30	8.6	−	DNA repair	Nucleus
SERPINA3	Serpin peptidase inhibitor A3	112874	47,621	99.88	7.24–7.54	++, +++	Acute phase response	Nucleus
SERPINC1	Serpin peptidase inhibitor C1	113936	52,569	100	6.32	+++	Blood coagulation	Extracellular
SLIRP	SRA stem-loop-interacting RNA-binding protein	74762723	12,341	23.70	10.25	+	Transcription	Mitochondria
SMC1A	Structural maintenance of chromosomes protein 1A	29336622	143,144	95.71	7.51	+++	DNA repair	Nucleus

TABLE I—*continued*

Gene name	Protein name	Swiss-Prot GI number	Protein molecular mass (kDa)	Protein score (%)	Protein pI	Carbonylation	Biological/molecular function	Cellular location
TMF1	TATA modulatory factor 1	218511858	122,767	65.13	4.88	–	Transcription regulation	Nucleus
TRIB1	Tribbles homolog 1	83305929	40,983	99.16	6.86	–	Response to LPS	Cytoplasm
VCL	Vinculin	21903479	123,722	97.36	5.5	+++	Muscle contraction	Extracellular
VIM	Vimentin	149021116	58,000	92.15	9.8	–	Host-pathogen interaction	Cytoplasm
ZBTB43	Zinc finger and BTB-43	23396976	52,597	90.40	5.46	–	NA	NA
ZNF248	Zinc finger protein 248	47606299	67,044	78.50	8.59	–	Transcription regulation	Nucleus
ZNF840	Zinc finger protein 840	218512159	83,181	83.31	9.69	–	Transcription regulation	Nucleus
FLJ45035	Uncharacterized protein	74710968	15,488	95.19	7.41	–	NA	NA

pH 3–10 and pH 4–9 IPG strips, high abundance sera proteins resolved in the middle portion or on the acidic side of the second dimension 8–16% gradient gel (supplemental Fig. S6, *A* and *B*). The narrow range IPG strips (pH 4–7) provided an enhanced resolution of high abundance sera proteins and detection of 5-fold more spots than were detected by using pH 3–10 and pH 4–9 IPG strips (supplemental Fig. S6*C*). We therefore used pH 4–7 IPG strips for further analysis of high abundance protein sera fractions of normal controls, seropositive chagasic subjects, and cardiomyopathy patients of other etiologies. High abundance protein fractions were pooled (three subjects/sample), and at least six samples/group were resolved to obtain 6 gel replicas per group. Representative gel images for each group are shown in Fig. 4 (*A–D*). Gel images were aligned by using Progenesis SameSpots™, and densitometric analysis was performed to select differentially expressed protein spots (Fig. 4*E*). MALDI-TOF MS/MS analysis of 32 protein spots that were differentially expressed in chagasic patients by ≥5-fold as compared with normal controls ($p_{ANOVA} \leq 0.01$) yielded 71 protein identifications (Table II). Further, we identified 14 low abundance proteins that partitioned with high abundance proteins in a disease-specific manner (Table II).

Carbonyl Proteome Profile in Chagas Patients—In prior investigations in our lab, we have shown that the progression of Chagas disease is associated with pathologic oxidative stress. To investigate whether oxidative protein modifications elicit a disease specific serum carbonyl proteome, we incubated the high and low abundance protein sera fractions with DNPH and then performed one-dimensional gel electrophoresis/immunoblotting to detect the DNPH-derivatized carbonyl proteins (supplemental Fig. S7). These data showed that a large number of low abundance (supplemental Fig. S7*A*) sera proteins in seropositive/chagasic and other cardiomyopathy subjects were oxidized when compared with those noted in normal controls. The extent of high abundance protein oxidation was more pronounced in chagasic subjects than that noted in other cardiomyopathy patients (supplemental Fig. S7*B*). To facilitate the identification of oxidized proteins, sera fractions containing high abundance proteins were resolved by 2D-GE, and WB was performed by using anti-DNPH antibody (Fig. 5, *A–C*). Comparisons of 2D/WB membrane images identified numerous oxidatively modified protein spots in high abundance protein sera fractions from chagasic and other cardiomyopathy subjects (Fig. 5). We also found through comparative analysis of signal densities from SYPRO Ruby-stained gels (Fig. 4) and Western blotting images (Fig. 5) that a majority of oxidized proteins in high abundance protein sera fractions from chagasic subjects were also differentially expressed. In addition to several of the high abundance proteins (albumin, transferring, IgH, IgL), we submitted six protein spots that were oxidized in chagasic samples (marked by *arrows*, Fig. 5*C*) to MALDI-TOF MS/MS analysis for protein identification. Oxidized proteins are marked by footnote *a* in (Table II).

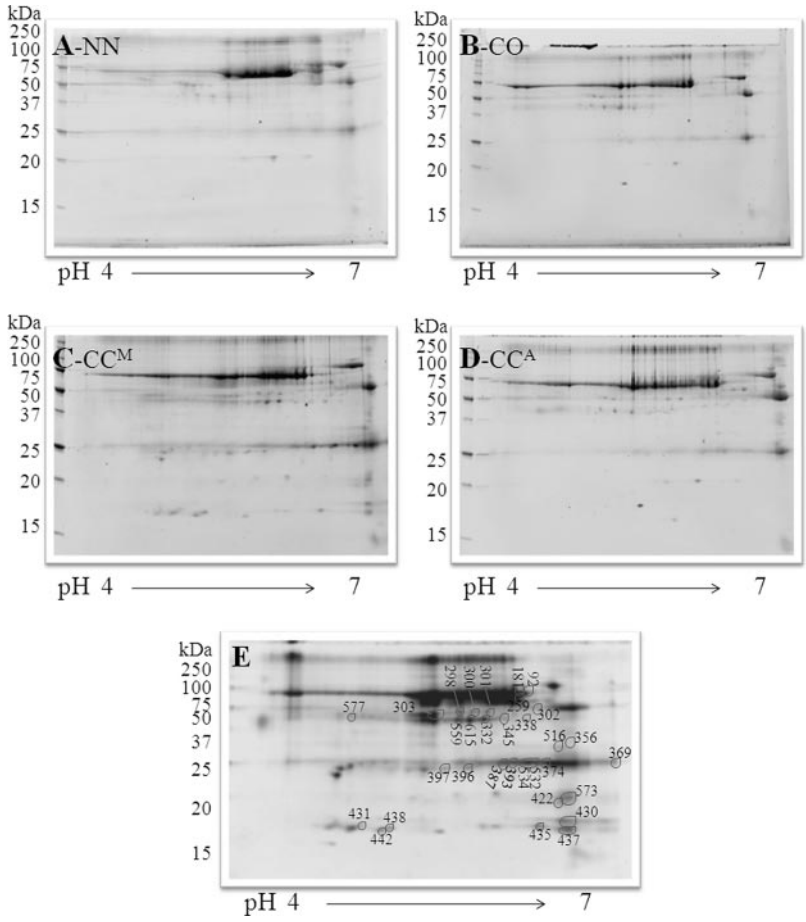

FIG. 4. **2D-GE analysis of serum fractions containing high abundance proteins.** *A–D*, IgY-12 high capacity LC10 proteome partitioning system was employed to fractionate high abundance sera proteins from normal subjects exhibiting no disease (*A*), patients exhibiting cardiomyopathy of other etiologies (*B*), and seropositive chagasic (CC) individuals from Argentina (*C*) and Mexico (*D*). High abundance proteins containing sera fractions were run in the first dimension by isoelectric focusing on 11-cm linear pH 4–7 IPG strips, and second dimension was carried out by SDS-PAGE on an 8–10% gradient gel. Shown are Sypro Ruby-stained gel images. *E*, protein spots, marked on *C*, that were identified to be differentially expressed by >2-fold in chagasic subjects were submitted to MALDI-TOF MS analysis (listed in Table II).

For the identification of oxidized proteins in low abundance protein-enriched sera fractions, second dimension protein fractions from PF2D analysis were resolved on 8% acrylamide gels, and WB was performed with anti-DNPH antibody. Shown in Fig. 5*D* is a typical SDS-PAGE/WB analysis of ProteomeLab second dimension fractions from a seropositive/chagasic subject. Corresponding Sypro Ruby-stained gels (shown as *inset* in Fig. 3) were utilized to cut gel slices for MALDI-TOF MS analysis and identification of oxidized low abundance sera proteins. These analyses led to identification of 33 oxidatively modified, low abundance proteins in chagasic subjects as compared with normal controls (listed in Table I).

IPA Network Analysis of the Disease-associated Proteome Signature—The differentially expressed (or oxidized) protein data sets (Tables I and II) were submitted to IPA and UniProt for identifying cellular localization and molecular and biological function. As expected for sera, >42% of the proteins differentially expressed in chagasic patients were extracellular (supplemental Fig. S8). Detection of the increased release of proteins belonging to cellular compartments, including the cell cytoplasm (13%) and nucleus (10%) in chagasic sera (supplemental Fig. S8) indicated that *T. cruzi*-induced cellular events and cell injury/cell death, and the resultant release of intracellular proteins, at least partially, contribute to disease-specific differential sera proteomes.

Following IPA analysis of the differentially expressed proteins in cardiomyopathy patients, we identified four major associated networks (supplemental Table S1). These included: 1) cellular assembly and organization related to cardiovascular diseases (22 proteins, supplemental Fig. S9.1); 2) cardiovascular system development and function (20 proteins, supplemental Fig. S9.2); 3) lipid metabolism, molecular transport and small molecule biochemistry (12 proteins, supplemental Fig. S9.3); and 4) tissue development, gene expression, cardiovascular disease (10 proteins, supplemental Fig. S9.4). Overlay of the associated networks (supplemental Table S1) identified CLU, KNG1, and PLG as central nodes (supplemental Fig. S9.5). Functional analysis by IPA identified that 29 of the differentially expressed proteins, including 14 of the 22 proteins linked to cellular assembly and organization related to cardiovascular diseases network, were responsible for elicitation of inflammation and an immune response (supplemental Table S2). These included molecules indicative of changes in activation of leukocytes (C4B, F2, GC, IGHG1, IGHG3, KNG1, PLG, PRL, and SERPING1), a quantity of phagocytes (BCL2A1, GCNT1, MYH11, PLG, PRL, and TF), movement, migration, and activation of phagocytes or neu-

TABLE II

Proteome profile of high abundance protein sera fractions in human patients with cardiomyopathy of chagasic and other etiologies

The high abundance proteins in human sera samples from normal healthy subjects and chagasic and other cardiomyopathy patients were separated from low abundance proteins using IgY-12 high capacity LC10 proteome partitioning chromatography and resolved by a 2D-GE approach. The gel images were analyzed on Progenesis SameSpotst™ software, and normalized spot volumes were used for comparison of the two groups. Proteins spots with >2-fold change in chagasic sera were subjected to MALDI-TOF MS/MS analysis. The putative molecular/biological function and cellular location were identified using ingenuity pathway analysis and UniProt software. NA, no match available in public information databases.

Spot No.	Gene name	Protein name	Swiss-Prot No.	Molecular mass (kDa)	Protein score	pI	Molecular/biological function	Cellular location
256, 257, 297, 301, 332[a], 344, 374[a], 396, 397, 400, 401, 445, 486, 487, 488, 505, 572, 614[a]	ALB	Albumin	113576	69,321.5	99–100	5.92	Transport, Antioxidative	Extracellular
297	MTHFD1	C-1-Tetrahydrofolate synthase	115206	101,495.3	81.27	6.89	Oxidoreductase	Mitochondria
332	CNOT10	CCR4-NOT transcript ion complex subunit 10	74733982	82,257.5	75.87	7.95	Protein binding, mRNA metabolism	Cytosol
487	C1R	Complement C1r	218511956	80,066.8	92.19	5.82	Peptidase/immune response	Extracellular
297, 505	FGG	Fibrinogen γ	20178280	51,478.9	100	5.37	Protein binding/Signal transduction	Extracellular
505	HSDL2	Hydroxysteroid dehydrogenase-like 2	74749521	45,365.5	70.32	8.07	Oxidoreductase	Mitochondrion
257, 438, 442, 500, 505, 528, 582, 600, 612	IGHG1	Ig γ1 chain C	121039	36,083.2	92.37–100	8.46	Antigen binding/immune response	Extracellular
442[a], 500, 505, 528, 582, 600, 612	IGHG2	Ig γ2 chain C	218512079	35,877.8	76.96–100	7.66	-do-	-do-
438, 442[a], 500, 505, 528, 582, 600, 612	IGHG3	Ig γ3 chain C	193806361	41,260.4	81.27–100	8.23	-do-	-do-
374[a]	IGKC	Ig κ chain C region	125145	11,601.7	99.91	5.58	-do-	-do-
517, 528, 612	KRT1	Keratin, cytoskeletal 1	238054406	65,999	100	8.15	-do-	-do-
528	KRT2	Keratin, cytoskeletal 2	239938650	65,393.2	100	8.07	-do-	-do-
486, 612	KRT9	Keratin, cytoskeletal 9	239938886	62,026.8	99.89	5.14	-do-	-do-
517, 528	KRT10	Keratin, cytoskeletal 10	269849769	58,791.7	100	5.13	Protein binding/epidermis	Intermediate fill
257	LRRK2	Leucine-rich repeat kinase 2	120892	285,873.9	89.47	6.34	ATP binding/oxidative stress response	Mitochondria
505	MSH4	MutS homolog 4	30316344	104,689.2	74.15	7.16	DNA repair	Nucleus
445, 517	NRAP	Nebulin-related anchoring protein	115502505	196,950.3	82.92	9.24	Ribosomal biogenesis	Nucleus
517	PVALB	Parvalbumin α	131100	12,051	99.38	4.98	Ca^{2+} binding	Cytoplasm
297	PCID2	PCI domain-containing protein 2	85681034	45,999.8	99.18	8.78	Protein binding/apoptosis inhibition	–
438	PRODH	Proline dehydrogenase	119364639	59,192.8	77.48	6.43	Oxidoreductase	Mitochondria
156	LOC442122	Uncharacterized protein	74710968	15,487.5	90.17	7.41	Immune response	NA
156[a], 301	TF	Serotransferrin	7018	76,999.6	100	6.81	Transport	Extracellular
528	UTRN	Utrophin	215274104	394,220.2	73.55	5.2	Actinin binding/muscle development	Nucleus
374[a]	ZNF615	Zinc finger protein 615	161784348	83,684.2	71.65	9.35	DNA binding/Transcription	Nucleus
396	ZNF528	Zinc finger protein LOC400713	172046155	66,719.2	70.99	9.45	-do-	-do-
505	ZSWIN2	Zinc finger SWIM domain-protein 2	151112	72,673.9	84.42	8.93	Zn^{2+} binding/apoptosis	NA

[a] Selected, differentially expressed proteins that were recognized by Western blotting with anti-DNPH antibody and consisted DNPH-derivatized carbonyl adducts.

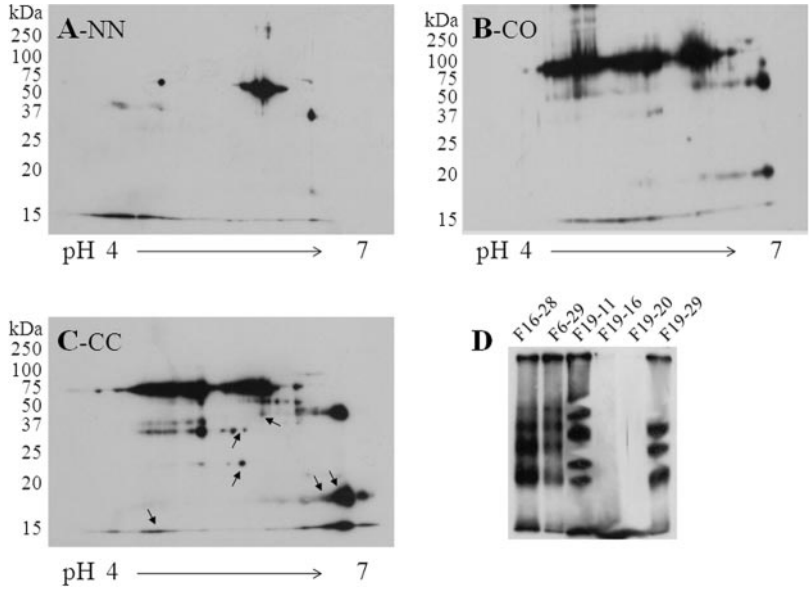

FIG. 5. **Protein carbonyls detected in serum of chagasic subjects.** *A–C*, high abundance proteins containing sera fractions (separated by using the IgY-12 columns) from normal subjects (*A*), patients exhibiting cardiomyopathy of other etiologies (*B*), and seropositive chagasic individuals (*C*) were run in the first dimension by isoelectric focusing on 11-cm linear pH 4–7 IPG strips. The strips were incubated with DNPH to derivatize carbonyl proteins, and second dimension was carried out by SDS-PAGE on an 8–10% gradient gel. Shown are the representative images of Western blotting with anti-DNPH antibody. Respective Sypro Ruby-stained gel images are shown in Fig. 4. *D*, for the detection of protein carbonyls in low abundance sera protein fractions, PF2D second dimension fractions were derivatized with DNPH and then subjected to fourth dimension fractionation on an 8% polyacrylamide gel. Western blotting was performed with anti-DNPH antibody. The Coomassie Blue-stained image is shown as an *inset* in Fig. 3. Carbonyl proteins were identified by MALDI-TOF MS analysis (listed in Tables I and II).

trophils (ALB, C4B, CFB, F2, GC, GCNT1, IGHG1, IGHG3, KNG1, PLG, PRL, and SERPING1), oxidative burst of granulocytes, cytotoxic reactions (IGHA1, IGHA2, IGHG1, IGKC, and IGHG3), and aggregation of blood platelets (ALB, F2, GC, KNG1, PLG, and SERPINC1). Functional analysis of the cardiovascular system development and function network merged with cardiovascular disease category annotated the differentially expressed proteins to thrombosis (ALB, CFB, F2, HRG, KNG1, PLG, and SERPINC1), angiogenesis (F2, HRG, KNG1, MEF2C, PLG, PRL, SERPINC1, and VIM), and vasodilatation (APOC3, F2, K2, KNG1, PLG, PRL, and VIM) of blood vessel or aorta, increased permeability (C4B, F2, KNG1, and SERPINC1) or formation (FGG, KNG1, MEF2C, MYH11, PLG, and PRL) of blood vessels, capillary and endothelial tubes, and muscle contraction (C4B, KNG1, MYH11, MYL2, UTRN, and VCL). The differentially expressed proteins (n = 23) in lipid metabolism and molecular transport category were functionally annotated to affect lipid quantity (ALB, APOC3, CLU, F2, GC, F2R, KNG1, PLG, PRL, PVALB, SERPINC1, and TTR) via altering lipid synthesis (ALB, CLU, CYP1B1, F2, KNG1, PLG, POMC, and PRL) or degradation (ALB, APOC3, CLU, PLG), and to lipid release (ALB, F2, KNG1, PLG, PRL, SERPINC1, and VIM) or transport (ALB, APOC3, CLU, F2, and GC). Further, we identified 30 differentially expressed proteins that were linked to cell death and apoptosis (supplemental Table S2). The top canonical pathway analysis identified several differentially expressed proteins (ALB, AMBP, C1R, C4B, C4BPA, CFB, CP, F2, FGG, HRG, ITIH2, PLG, SERPINA3, SERPING1, TF, and TTR) that were indicative of the acute phase response signaling pathway (supplemental Fig. S10) and that can be induced in response to infection or triggered by tissue injury and provide protection by using nonspecific defense mechanisms.

Validation of Differentially Expressed Proteins in Chagas Disease—To validate the *T. cruzi*-induced differential expression of sera proteins identified by PF2D/2D-GE and mass spectrometry, we chose to perform ELISA with protein-specific antibody to detect the expression levels of VCL, MYL2, VIM, and PLG in chagasic (n = 35) and healthy subjects (n = 20) (Fig. 6). These data exhibited a substantially higher level of VCL, MYL2, and PLG in seropositive chagasic patients compared with normal healthy controls ($p < 0.001$). We noticed that ~51% of the chagasic patients exhibited VCL levels significantly higher than the $\text{mean}_{\text{seropositive}}$ values (mean $A_{450\ \text{nm}}$, 0.372 ± 0.114 *versus* 0.186 ± 0.053; range, 0.240–0.499 *versus* 0.101–0.412, seropositive *versus* seronegative, $p < 0.001$; Fig. 6*A*). Likewise, 56% of the chagasic patients exhibited a significantly higher level of MYL2 than the $\text{mean}_{\text{seropositive}}$ value (mean $A_{450\ \text{nm}}$, 0.329 ± 0.101 *versus* 0.173 ± 0.0181; range, 0.121–0.332 *versus* 0.204–0.423; seropositive *versus* seronegative, $p < 0.0001$; Fig. 6*B*). Further, the sera level of PLG was significantly increased in 32% of the chagasic patients (mean value, 216 ± 33 *versus* 188 ± 40; range, 147–280 *versus* 100–220 μg/ml; seropositive *ver-*

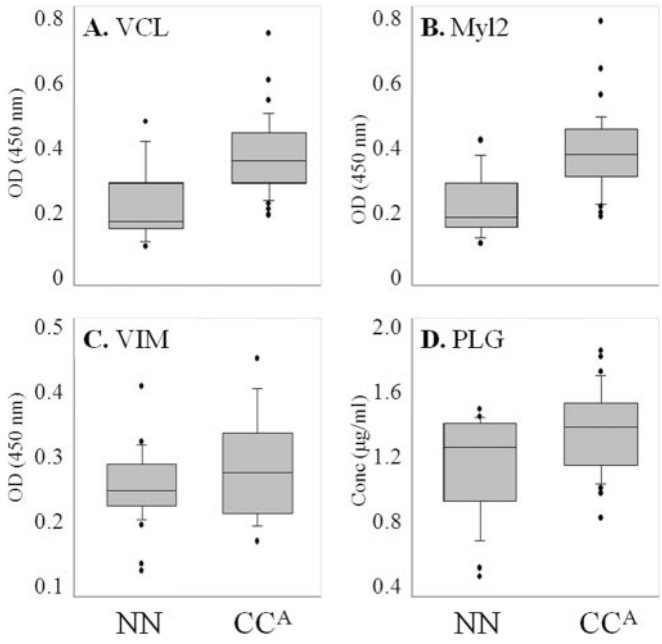

FIG. 6. **Validation of expression profile of selected proteins in chagasic sera.** Whole sera samples from normal and chagasic subjects were subjected to ELISA analysis by using antibodies against VCL (*A*), cardiac specific MYL2 (*B*), VIM (*C*), and PLG (*D*). Standard deviation for triplicate observations for each sample was <12%. Shown is box plot of ELISA data, graphically depicting the values for seronegative and seropositive groups. The *horizontal lines* of the box (*bottom* to *top*) depict the lower quartile (Q1, cuts off lowest 25% of the data), median (Q2, middle value), and upper quartile (Q3, cuts off the highest 25% of the data). The *lower* and *upper whiskers* depict the smallest and largest non-outlier observations, respectively, and the *solid dots* represent the outliers. The spacing between the different parts of the *box* indicates the degree of dispersion (spread). *Conc*, concentration; *OD (450 nm)*, $A_{450\ nm}$.

sus seronegative, $p < 0.0001$; Fig. 6*D*). The sera levels of VIM were increased in 10% of the seropositive individuals as compared with those in normal healthy controls (mean $A_{450\ nm}$, 0.329 ± 0.101 *versus* 0.173 ± 0.0181; range, 0.204–0.423 *versus* 0.121–0.332; seropositive *versus* seronegative; Fig. 6*C*); however, these results were not statistically significant. Seronegative patients with cardiac symptoms caused by other etiologies ($n = 25$) exhibited a marginal, but not statistically significant, increase in VCL, and no increase in MYL2 and VIM levels in sera when compared with these levels in normal controls (data not shown). Together, these data validated the PF2D/mass spectrometry results and led us to suggest that the sera levels of VCL, MYL2, and PLG will be useful indicators of disease and disease severity in human chagasic patients.

DISCUSSION

In this study, we have developed a comprehensive serum proteome profile of chagasic human patients by utilizing a combination of PF2D ProteomeLab and traditional 2D-GE techniques. Parasite persistence and oxidative damage in the heart are known to be of pathological significance during Chagas disease (32, 33). To examine this, we collected sera of clinically diagnosed cardiomyopathy patients with or without Chagas disease and compared with normal healthy controls from the same geographic area to identify the disease-specific serum proteome changes. We identified 14 proteins that were differentially expressed in sera of other cardiomyopathy patients, and 80 and 26 proteins that were differentially expressed or oxidized, respectively, in the sera of chagasic patients. Functional and network analysis assigned a majority of the differentially expressed proteins to molecular pathways associated with inflammatory responses, lipid metabolism, and molecular transport, contributing to cell death and cardiovascular disease, *i.e.*, myocardial infarction, embolism, and hypertension, in chagasic patients. Canonical pathway analysis verified the disease association to dysregulation of the acute phase response signaling pathway. To the best of our knowledge, this is the first study demonstrating the serum oxidative and inflammatory response profile, and serum detection of cardiac proteins parallels the pathologic events contributing to Chagas disease development. Furthermore, we believe the findings have a potential utility in diagnosing disease severity and designing suitable therapy for management of human chagasic patients.

The PF2D system represents a promising tool for proteomic mapping because of its superior reproducibility, sensitivity, and automation capacity over the classical 2D gel electrophoresis, as demonstrated by a number of studies in various cell models and tissue types (34–38). The present work is the first demonstration of using such a protein fractionation technique for a large scale profiling of the serum proteome of chagasic patients. The 12 major proteins accounting for >90% of the serum protein interfere with the detection of low abundance potential biomarker proteins. The IgY LC10 chromatography removed 90–95% of the high abundance proteins allowing enrichment of low abundance proteins, yet proteome analysis of high abundance protein fractions by 2D-GE demonstrated that some of the low abundance proteins partitioned with high abundance protein sera fractions (Table II), likely because of binding of low abundance proteins to high abundance proteins. Overall, the PF2D analysis of low abundance protein fractions yielded highly reproducible data, leading to the identification of >80 disease-associated low abundance proteins ($p < 0.001$). Of these, some proteins were identified as differentially expressed in multiple groups. For example, C4BPA was identified to be differentially expressed in normal as well as chagasic patients because of the difference in oxidation; PCID2 was identified to be increased in the sera of chagasic and other cardiomyopathy patients as compared with normal controls, and HRG, SERPINA3, and NUMA1 were identified in different second dimension fractions of chagasic patients (Table I). A similar anomaly has been reported in previous proteomic studies in which the PF2D system was used (39–41). Several factors including time-based rather than peak-based

fractionation during second dimension chromatography and post-translational modifications, *e.g.*, protein carbonylation, phosphorylation resulting in a shift in their pI or molecular weight, may have contributed to variance in partitioning and detection of proteins.

IPA is highly curated and comprehensive software used for the integration of proteins into networks and pathways with biological meaning. Network analysis of serum proteome profiles of chagasic patients identified four major subnetworks linked to the host response to *T. cruzi* infection and disease development, three of which were directly indicative of alterations in gene expression, cellular assembly, and cardiovascular system development and function leading to cardiovascular disease (supplemental Table S1). Functional annotation associated 29 of the differentially expressed proteins to the inflammatory response category (supplemental Table S2), many of which are known to affect activation of leukocytes, quantity of phagocytes, movement and migration of phagocytes, and aggregation of blood platelets. The presence of a mixed host response, *i.e.*, attempt to decrease (*e.g.*, GCNT1, SERPINA3, SERPIC1, and SERPING1), as well as increase (*e.g.*, F2, GC, IGHA1, IGHA2, IGHG3, IGKC, KNG1, and PRL) immune responses was evident, which may indicate persistence of inflammation, known to be of pathological significance in Chagas disease (42, 43). Overall, it appeared that increased complement activation (C4A/C4B, CLU, and KNG1) and activation and proliferation of phagocytes (F2, GC, KNG1, MYH11, PLG, and TF) and leukocytes (C4B, F2, GC, IGHG3, KNG1, PLG, and PRL) were followed by attempts to control cell movement or migration of immune cells (PLG, SERPINA3, SERPINC1, and SERPING1) to prevent tissue damage caused by inflammatory cytotoxic reactions. It is important to note that of the 29 differentially expressed inflammation-associated proteins (supplemental Table S2), seven proteins (ALB, BCL2A1, IGHG3, IGKC, SERPINA3, SERPINC1, and TF) were carbonylated (Tables I and II) in chagasic serum, which indicates that oxidative stress plays an important role in modulating the host immune response against *T. cruzi.* Other studies have demonstrated that ROS elicit inflammatory cytokines (*e.g.*, TNF-α, IFN-γ, and IL-1β) in cardiomyocytes infected by *T. cruzi* (44, 45). Inflammatory pathology was controlled in chronically infected experimental animals and human patients by enhancing the antioxidant status, which was also beneficial in preserving cardiac function during Chagas disease (15, 16, 46, 47). Our recent observations indicate that the mitochondrial release of ROS caused by electron transport chain dysfunction and enhanced release of electrons to molecular oxygen is the primary source of oxidative stress in the heart (13). Further studies will be required to delineate the significance of mitochondrial ROS and classical ROS producers, *i.e.*, NADPH oxidase and myeloperoxidase, known to play an important role in parasite control during the acute phase of infection (24, 49, 81), in elicitation of inflammatory responses during Chagas disease.

Twenty-three of the differentially expressed proteins in chagasic serum were allotted to the lipid metabolism/molecular transport category (supplemental Table S2). The expression levels of several of the proteins including ALB, APOC3, F2, F2R, KNG1, POMC, PRL, and SERPINC1 that increase quantity, production, release, and transport of lipids, specifically arachidonic acid and prostaglandins, were deregulated in chagasic patients (Tables I and II). Arachidonic acid is the precursor for prostaglandins, which function as autocrine and paracrine mediators that act upon several cell types including platelets and endothelium (50). Heightened platelet reactivity and endothelial cell dysfunction associated with an increased release of 6-keto-prostaglandin F1α from endothelium during *T. cruzi* infection is documented (51) and supported by our observation of the increased expression of several proteins (ALB, F2, GC, KNG1, and SERPINC1) activated to control blood platelet aggregation. Host as well as parasite-derived prostaglandins have been implicated in the pathogenesis of Chagas disease (52), and eicosanoids present during acute infection have been suggested to act as immunomodulators (52) aiding the transition to and maintenance of the chronic phase of the disease (53, 54). Treatment with cycloxygenase 2 inhibitors (*e.g.*, aspirin) has been shown to reduce cardiac damage (54) in chagasic experimental models. Our data in this study validate the observations made in experimental models and allow us to propose that dysregulation of lipid mediators and inflammation are interlinked pathological events during human Chagas disease, to be further validated in future studies.

When categorized in relation to disease severity, it became apparent that chagasic patients exhibited proteome signatures of cardiovascular disorders (CFB, CTTN, DIP2A, GMDS, HRG, KIAA1370, MYH11, OSBPL8, PDE4A, PLG, SERPINC1, TRIB1, and VCL) associated with myocardial ischemia (DIP2A, GMDS, KIAA1370, MYH11, OSBPL8, PDE4A, PLG, SERPINC1, and VCL) and cardiomyopathy (PLG, TRIB1, and VCL). The proteomic signature of merged networks of Chagas disease positioned PLG (plasminogen) and F2 (prothrombin) at a central nodal position (supplemental Fig. S9.5) with connectivity to numerous proteins indicative of thrombosis (ALB, CFB, F2, HRG, KNG1, PLG, and SERPINC1), angiogenesis (F2, HRG, KNG1, MEF2C, PLG, PRL, and SERPINC1), vasodilatation of blood vessel or aorta (APOC3, F2, K2, KNG1, PLG, PRL, and VIM), increased permeability of blood vessel and endothelial tubes (C4B, F2, KNG1, and SERPINC1), and muscle loss of contraction (C4B, KNG1, MYH11, MYL2, UTRN, and VCL). Moreover, indicators of platelet aggregation (ALB, F2, GC, KNG1, PLG, and SERPINC1) and complement activation (C4B, CFB, CLU, IGHG1, and KNG1), as well as acute phase response signaling (ALB, AMBP, TTR, CFB, HRG, TF, ITIH2, C4BP, C4, FGG, CP, SERPINA2, SERPING1, and SERPINF), were linked to PLG and/or F2 nodes. PLG, when activated to function as serine protease (plasmin), directly attacks fibrin blood clots (55). Prothrombin (coaglulation

factor II) is proteolytically activated to form thrombin that acts as a trypsin-like serine protease. F2 complements PLG function, contributing platelet activation and aggregation via activation of protease-activated receptors on the cell membranes and catalyzing polymerization of soluble fibrinogen into insoluble fibrin (56). A deficiency of, as well as up-regulation of, PLG and F2 beyond physiological levels can lead to multiple pathological outcomes, including thrombosis caused by partial or inadequate degradation of blood clots, defective wound healing, and excessive bleeding (55–57). Plasmin is postulated to influence the progression of cardiovascular diseases through activation of collagenases and matrix metalloproteinases and resultant degradation of matrix proteins (58) and has also been implicated in metabolic syndrome (59). PLG, F2, and their receptors are also closely linked to regulation of cardiovascular inflammatory responses and have been suggested by others to influence cell migration through regulation of growth factor and chemokine pathways and acute phase response signaling through activation of C3 component of complement system (60). Plasmin-mediated fibrin degradation products have vascular permeability-inducing effects and are considered a cardiovascular disease risk factor in aging (61). An increase in thrombolytic risk factors is documented in chagasic patients (62). Our network analysis provides the first indication of the central role of PLG and F2 in Chagas disease. Dissection of the mechanisms altered by PLG and F2 in an effort to understand their roles *in vivo* represents a future challenge in unraveling the pathogenesis of Chagas disease.

In prior studies, we and others have documented oxidative stress pathogenesis in experimental models of Chagas disease (32, 33) and shown that enhancing antioxidant status was beneficial in controlling cardiac tissue damage and subsequent loss of contractile function (16). In this study, five proteins associated with free radical scavenging, *i.e.*, ALB, CLU, CP, F2, and PRODH were identified, all of which were either depressed or oxidized in chagasic patients. CLU (Clustrin) is suggested to prevent cell death and the associated cytotoxicity of superoxide (63), and CP (ceruloplasmin) is related to reduction of superoxide through its antioxidant properties independently of its function in iron metabolism (64). A positive correlation between ceruloplasmin and the incidence of atrial fibrillation has been documented in a population-based cohort study (65). PRODH (proline dehydrogenase) modulates the intracellular redox environment and protects mammalian cells against oxidative stress (66). Albumin is present in large amounts in plasma and sera, and 70–80% of Cys^{34} in albumin contains a free sulfhydryl group. Through the reduced Cys^{34}, ALB is able to scavenge hydroxyl radicals (67). Cys^{34} and Met residues (six) are also oxidation-sensitive amino acids in ALB. Increased glycation of ALB occurs in diabetes mellitus, which is one of the pathological conditions associated with an early occurrence of vascular complications (68). Our observation of the decreased expression or increased oxidation of these proteins in chagasic patients provides the proteomic signature of compromised antioxidant status.

Four proteins (VIM, MYL2, MYH11, and VCL) directly linked to cardiac muscle functions deserve to be further discussed. VIM is a member of the intermediate filament network, and along with microtubules and actin microfilaments, it plays an important role in maintaining cell shape and integrity of cytoplasm and stabilizing cytoskeletal interactions (69). Vimentin is also shown to be localized in common carotid artery and heart valves and serves as a target antigen of peripheral and heart-infiltrating T cells during valvular disease (70). The increased detection of VIM in the heart is indicative of the occurrence of a fibrotic process, because infiltrating fibroblasts replace damaged cardiomyocytes in disease conditions (70) and has been identified by proteomic inventory of myocardial proteins in patients with Chagas disease (71). The increased plasma detection of VIM in 10% of the seropositive chagasic patients may be indicative of its significance in relation to disease severity and requires further investigation in large cohort studies. MYL2 is a cardiac-specific protein. MYL2 dimerizes with cardiac myosin β (or slow) heavy chain, and its phosphorylation by Ca^{2+} triggers cardiac contractions. Mutations in *MYL2* or abnormalities in MYL2 expression are associated with cardiomyopathy (72), heart failure (73), left ventricular hypertrophy (74), and familial hypertrophy (75). MYH11 is a smooth muscle myosin belonging to the myosin heavy chain family. It functions as a major contractile protein, utilizing the energy of ATP hydrolysis to move actin filaments and produce muscle force. MYH11 mutations are documented to result in a distinct aortic and occlusive vascular pathology (76). Deletion, splicing, and mis-sense mutations in MYH11 have been identified in patients with familial thoracic aortic aneurysm and dissections with patent ductus arteriosus type 4, which is one of the most severe cardiovascular conditions in adults (77). Studies have shown that MYH11 heterozygous mutations lead to early severe decrease in the elasticity of the aortic wall, a finding consistent with the role of smooth muscle cells in maintaining the mechanical properties of the thoracic aorta (78). Vinculin plays a pivotal role in cell adhesion and migration by providing the link between the actin cytoskeleton and the transmembrane receptors integrin and cadherin (79). VCL is a cytoskeletal protein associated with cell to cell and cell-matrix junctions, where it is thought to function as one of several interacting proteins involved in anchoring F-actin to the membrane. Defects in VCL are the cause of dilated cardiomyopathy (80). The absence of VCL demonstrates a decrease in the spreading of cells that was accompanied by reduced stress fiber formation and restored by its overexpression (48). The sera release of MYL2 and MYH11 and up-regulation of VCL provide a comprehensive set of biomarkers of cardiac muscle injury and development of clinical Chagas disease in human patients.

In summary, we were successful in employing PF2D and 2D-GE to resolve low abundance and high abundance sera

proteins for the development of a proteomic signature of Chagas disease. The functional analysis of differentially expressed/oxidized sera proteins suggested that dysregulated inflammation/acute phase response signaling and lipid metabolism relevant to production of prostaglandins were associated with cell death and cardiovascular disease in chagasic patients. Further studies are required to investigate the causal and mechanistic relationship of altered lipid metabolism in Chagas disease. Our ability to detect significantly higher levels of MYL2, VCL, and PLG in the sera of chagasic subjects indicates that these protein biomarkers are independent of the parasite lineage and the genetic or ethnic background of the host and thus have potential utility for diagnosis of cardiac muscle injury and development of clinical Chagas disease in human patients. These results provide an impetus for biomarker validation in large cohorts of clinically characterized chagasic patients.

Acknowledgments—We appreciate the consistent and long standing support of Dr. Ines Vidal, Eduardo Ledesma, Graciela Costello, Miriam Aramayo, Jimena Guanuco, and Veronica Saldaño at the Central Laboratory of San Bernardo Hospital (Salta, Argentina) with patient recruitment, serology tests, and patient categorization. Our thanks are also due to Marley Cabalerro for help with ELISA. We are thankful to the Biomedical Resource Facility and the Mass Spectrometry Laboratory at the University of Texas Medical Branch at Galveston for mass spectrometric analysis.

* This work was supported in part by NHLBI, National Institutes of Health Grants HL088230 and HL094802 (to N. J. G.).

[S] This article contains supplemental material.

** To whom correspondence should be addressed: 3.142C Medical Research Bldg., University of Texas Medical Branch, 301 University Blvd., Galveston TX 77555-1070. Tel.: 409-747-6865; Fax: 409-747-6869; E-mail: nigarg@utmb.edu.

REFERENCES

1. Chagas disease: A neglected emergency. (2009) *Lancet* **373,** 1820
2. World Health Organization (2010) Chagas disease: Control and elimination. UNDP/World Bank/WHO, http://apps.who.int/gb/ebwha/pdf_files/WHA63/A63_17-en.pdf
3. Bern, C., and Montgomery, S. P. (2009) An estimate of the burden of Chagas disease in the United States. *Clin. Infect. Dis.* **49,** e52–e54
4. World Health Organization (2006) Report of the scientific working group on Chagas disease. UNDP/World Bank/WHO, http://www.who.int/tdr/diseases/chagas/swg_chagas.pdf
5. Marin-Neto, J. A., Cunha-Neto, E., Maciel, B. C., and Simões, M. V. (2007) Pathogenesis of chronic Chagas heart disease. *Circulation* **115,** 1109–1123
6. Saravia, S. G., Haberland, A., Bartel, S., Araujo, R., Valda, G., Reynaga, D. D., Ramirez, I. D., Borges, A. C., Wallukat, G., and Schimke, I. (2011) Cardiac troponin T measured with a highly sensitive assay for diagnosis and monitoring of heart injury in chronic Chagas disease. *Arch. Pathol. Lab. Med.* **135,** 243–248
7. Sabatine, M. S., McCabe, C. H., Morrow, D. A., Giugliano, R. P., de Lemos, J. A., Cohen, M., Antman, E. M., and Braunwald, E. (2002) Identification of patients at high risk for death and cardiac ischemic events after hospital discharge. *Am. Heart J.* **143,** 966–970
8. Stanley, B. A., Gundry, R. L., Cotter, R. J., and Van Eyk, J. E. (2004) Heart disease, clinical proteomics and mass spectrometry. *Dis. Markers* **20,** 167–178
9. Rassi, A., Jr., Rassi, A., Little, W. C., Xavier, S. S., Rassi, S. G., Rassi, A. G., Rassi, G. G., Hasslocher-Moreno, A., Sousa, A. S., and Scanavacca, M. I. (2006) Development and validation of a risk score for predicting death in Chagas' heart disease. *N. Engl. J. Med.* **355,** 799–808
10. Rassi, A., Jr., Rassi, A., and Marin-Neto, J. A. (2010) Chagas disease. *Lancet* **375,** 1388–1402
11. Wen, J. J., Vyatkina, G., and Garg, N. (2004) Oxidative damage during chagasic cardiomyopathy development: Role of mitochondrial oxidant release and inefficient antioxidant defense. *Free Radic. Biol. Med.* **37,** 1821–1833
12. Wen, J. J., Dhiman, M., Whorton, E. B., and Garg, N. J. (2008) Tissue-specific oxidative imbalance and mitochondrial dysfunction during *Trypanosoma cruzi* infection in mice. *Microbes Infect.* **10,** 1201–1209
13. Wen, J. J., and Garg, N. J. (2008) Mitochondrial generation of reactive oxygen species is enhanced at the Q_o site of the complex III in the myocardium of *Trypanosoma cruzi*-infected mice: Beneficial effects of an antioxidant. *J. Bioenerg. Biomembr.* **40,** 587–598
14. Wen, J. J., and Garg, N. J. (2010) Mitochondrial complex III defects contribute to inefficient respiration and ATP synthesis in the myocardium of *Trypanosoma cruzi*-infected mice. *Antioxid. Redox. Signal.* **12,** 27–37
15. Wen, J. J., Bhatia, V., Popov, V. L., and Garg, N. J. (2006) Phenyl-α-*tert*-butyl nitrone reverses mitochondrial decay in acute Chagas disease. *Am. J. Pathol.* **169,** 1953–1964
16. Wen, J. J., Gupta, S., Guan, Z., Dhiman, M., Condon, D., Lui, C., and Garg, N. J. (2010) Phenyl-α-*tert*-butyl-nitrone and benzonidazole treatment controlled the mitochondrial oxidative stress and evolution of cardiomyopathy in chronic chagasic rats. *J. Am. Coll. Cardiol.* **55,** 2499–2508
17. Stein, R. C., and Zvelebil, M. J. (2002) The application of 2D gel-based proteomics methods to the study of breast cancer. *J Mammary Gland Biol. Neoplasia* **7,** 385–393
18. Van den Bergh, G., and Arckens, L. (2005) Recent advances in 2D electrophoresis: An array of possibilities. *Expert Rev. Proteomics* **2,** 243–252
19. Imai, K., Koshiyama, A., and Nakata, K. (2011) Towards clinical proteomics analysis. *Biomed. Chromatogr.* **25,** 59–64
20. Levreri, I., Musante, L., Petretto, A., Bruschi, M., Candiano, G., and Melioli, G. (2005) Separation of human serum proteins using the Beckman-Coulter PF2D system: Analysis of ion exchange-based first dimension chromatography. *Clin. Chem. Lab. Med.* **43,** 1327–1333
21. Shin, Y. K., Lee, H. J., Lee, J. S., and Paik, Y. K. (2006) Proteomic analysis of mammalian basic proteins by liquid-based two-dimensional column chromatography. *Proteomics.* **6,** 1143–1150
22. Deford, J. H., Nuss, J. E., Amaning, J., English, R. D., Tjernlund, D., and Papaconstantinou, J. (2009) High-throughput liquid-liquid fractionation of multiple protein post-translational modifications. *J. Proteome Res.* **8,** 907–916
23. The Criteria Committee of the New York Heart Association (1994) *Nomenclature and Criteria for Diagnosis of Diseases of the Heart and Great Vessels*, 9th Ed., pp. 253–256, Little, Brown & Co., Boston, MA
24. Dhiman, M., Estrada-Franco, J. G., Pando, J. M., Ramirez-Aguilar, F. J., Spratt, H., Vazquez-Corzo, S., Perez-Molina, G., Gallegos-Sandoval, R., Moreno, R., and Garg, N. J. (2009) Increased myeloperoxidase activity and protein nitration are indicators of inflammation in chagasic patients. *Clin. Vaccine Immunol.* **16,** 660–666
25. Dhiman, M., Nakayasu, E. S., Madaiah, Y. H., Reynolds, B. K., Wen, J. J., Almeida, I. C., and Garg, N. J. (2008) Enhanced nitrosative stress during *Trypanosoma cruzi* infection causes nitrotyrosine modification of host proteins: Implications in Chagas' disease. *Am. J. Pathol.* **173,** 728–740
26. Berger, F., De Meulder, B., Gaigneaux, A., Depiereux, S., Bareke, E., Pierre, M., De, Hertogh, B., Delorenzi, M., and Depiereux, E. (2010) Functional analysis: Evaluation of response intensities: Tailoring ANOVA for lists of expression subsets. *BMC Bioinformatics* **11,** 510
27. Levine, R. L., Garland, D., Oliver, C. N., Amici, A., Climent, I., Lenz, A. G., Ahn, B. W., Shaltiel, S., and Stadtman, E. R. (1990) Determination of carbonyl content in oxidatively modified proteins. *Methods Enzymol.* **186,** 464–478
28. Wen, J. J., and Garg, N. (2004) Oxidative modifications of mitochondrial respiratory complexes in response to the stress of *Trypanosoma cruzi* infection. *Free Radic. Biol. Med.* **37,** 2072–2081
29. Yu, H. L., Chertkow, H. M., Bergman, H., and Schipper, H. M. (2003) Aberrant profiles of native and oxidized glycoproteins in Alzheimer plasma. *Proteomics* **3,** 2240–2248
30. Bouwman, F. G., de Roos, B., Rubio-Aliaga, I., Crosley, L. K., Duthie, S. J., Mayer, C., Horgan, G., Polley, A. C., Heim, C., Coort, S. L., Evelo, C. T., Mulholland, F., Johnson, I. T., Elliott, R. M., Daniel, H., and Mariman,

E. C. (2011) 2D-electrophoresis and multiplex immunoassay proteomic analysis of different body fluids and cellular components reveal known and novel markers for extended fasting. *BMC Med. Genomics* **4,** 24
31. Hu, S., Loo, J. A., and Wong, D. T. (2006) Human body fluid proteome analysis. *Proteomics* **6,** 6326–6353
32. Zacks, M. A., Wen, J. J., Vyatkina, G., Bhatia, V., and Garg, N. (2005) An overview of chagasic cardiomyopathy: Pathogenic importance of oxidative stress. *An. Acad. Bras. Cienc*. **77,** 695–715
33. Gupta, S., Wen, J. J., and Garg, N. J. (2009) Oxidative stress in Chagas disease. *Interdiscip. Perspect. Infect. Dis.* **2009,** 190354
34. Rabilloud, T., Chevallet, M., Luche, S., and Lelong, C. (2010) Two-dimensional gel electrophoresis in proteomics: Past, present and future. *J. Proteomics* **73,** 2064–2077
35. Li, X., Xiong, L., Xie, C., Cao, J., Deng, H., Lin, Y., Cao, R., Li, J., Chen, P., and Liang, S. (2010) Proteomics analysis of plasma membrane from liver sinusoidal endothelial cells after partial hepatectomy by an improved two-dimensional electrophoresis. *Mol. Cell Biochem.* **344,** 137–150
36. Suberbielle, E., Gonzalez-Dunia, D., and Pont, F. (2008) High reproducibility of two-dimensional liquid chromatography using pH-driven fractionation with a pressure-resistant electrode. *J. Chromatogr. B Analyt. Technol. Biomed. Life Sci.* **871,** 125–129
37. Skalnikova, H., Rehulka, P., Chmelik, J., Martinkova, J., Zilvarova, M., Gadher, S. J., and Kovarova, H. (2007) Relative quantitation of proteins fractionated by the ProteomeLab PF 2D system using isobaric tags for relative and absolute quantitation (iTRAQ). *Anal. Bioanal. Chem.* **389,** 1639–1645
38. Abdel-Hafeez, E. H., Kikuchi, M., Watanabe, K., Ito, T., Yu, C., Chen, H., Nara, T., Arakawa, T., Aoki, Y., and Hirayama, K. (2009) Proteome approach for identification of *Schistosomiasis japonica* vaccine candidate antigen. *Parasitol. Int*. **58,** 36–44
39. Chen, E. I., Hewel, J., Felding-Habermann, B., and Yates, J. R., 3rd. (2006) Large scale protein profiling by combination of protein fractionation and multidimensional protein identification technology (MudPIT). *Mol. Cell. Proteomics* **5,** 53–56
40. Pirondini, A., Visioli, G., Malcevschi, A., and Marmiroli, N. (2006) A 2-D liquid-phase chromatography for proteomic analysis in plant tissues. *J. Chromatogr. B Analyt. Technol. Biomed. Life Sci.* **833,** 91–100
41. Sheng, S., Chen, D., and Van Eyk, J. E. (2006) Multidimensional liquid chromatography separation of intact proteins by chromatographic focusing and reversed phase of the human serum proteome: Optimization and protein database. *Mol. Cell. Proteomics* **5,** 26–34
42. Kayama, H., and Takeda, K. (2010) The innate immune response to *Trypanosoma cruzi* infection. *Microbes Infect*. **12,** 511–517
43. Junqueira, C., Caetano, B., Bartholomeu, D. C., Melo, M. B., Ropert, C., Rodrigues, M. M., and Gazzinelli, R. T. (2010) The endless race between *Trypanosoma cruzi* and host immunity: Lessons for and beyond Chagas disease. *Expert Rev. Mol. Med*. **12,** e29
44. Gupta, S., Bhatia, V., Wen, J. J., Wu, Y., Huang, M. H., and Garg, N. J. (2009) *Trypanosoma cruzi* infection disturbs mitochondrial membrane potential and ROS production rate in cardiomyocytes. *Free Radic. Biol. Med.* **47,** 1414–1421
45. Ba, X., Gupta, S., Davidson, M., and Garg, N. J. (2010) *Trypanosoma cruzi* induces ROS-PARP-1-RelA pathway for up-regulation of cytokine expression in cardiomyocytes. *J. Biol. Chem.* **285,** 11596–11606
46. Ribeiro, C. M., Budni, P., Pedrosa, R. C., Farias, M. S., Parisotto, E. B., Dalmarco, E. M., Fröde, T. S., Oliveira-Silva, D., Colepicolo, P., and Filho, D. W. (2010) Antioxidant therapy attenuates oxidative insult caused by benzonidazole in chronic Chagas' heart disease. *Int. J. Cardiol*. **145,** 27–33
47. Souza, A. P., Jelicks, L. A., Tanowitz, H. B., Olivieri, B. P., Medeiros, M. M., Oliveira, G. M., Pires, A. R., Santos, A. M., and Araújo-Jorge, T. C. (2010) The benefits of using selenium in the treatment of Chagas disease: Prevention of right ventricle chamber dilatation and reversion of *Trypanosoma cruzi*-induced acute and chronic cardiomyopathy in mice. *Mem. Inst. Oswaldo Cruz* **105,** 746–751
48. Ezzell, R. M., Goldmann, W. H., Wang, N., Parashurama, N., and Ingber, D. E. (1997) Vinculin promotes cell spreading by mechanically coupling integrins to the cytoskeleton. *Exp. Cell Res.* **231,** 14–26
49. Guiñazú, N., Carrera-Silva, E. A., Becerra, M. C., Pellegrini, A., Albesa, I., and Gea, S. (2010) Induction of NADPH oxidase activity and reactive oxygen species production by a single *Trypanosoma cruzi* antigen. *Int. J. Parasitol*. **40,** 1531–1538
50. Smyth, E. M., Grosser, T., Wang, M., Yu, Y., and FitzGerald, G. A. (2009) Prostanoids in health and disease. *J. Lipid Res.* **50,** (suppl.) S423–S428
51. Tanowitz, H. B., Burns, E. R., Sinha, A. K., Kahn, N. N., Morris, S. A., Factor, S. M., Hatcher, V. B., Bilezikian, J. P., Baum, S. G., and Wittner, M. (1990) Enhanced platelet adherence and aggregation in Chagas' disease: A potential pathogenic mechanism for cardiomyopathy. *Am. J. Trop. Med. Hyg.* **43,** 274–281
52. Pinge-Filho, P., Tadokoro, C. E., and Abrahamsohn, I. A. (1999) Prostaglandins mediate suppression of lymphocyte proliferation and cytokine synthesis in acute *Trypanosoma cruzi* infection. *Cell. Immunol.* **193,** 90–98
53. Mukherjee, S., Machado, F. S., Huang, H., Oz, H. S., Jelicks, L. A., Prado, C. M., Koba, W., Fine, E. J., Zhao, D., Factor, S. M., Collado, J. E., Weiss, L. M., Tanowitz, H. B., and Ashton, A. W. (2011) Aspirin treatment of mice infected with *Trypanosoma cruzi* and implications for the pathogenesis of Chagas disease. *PLoS One* **6,** e16959
54. Abdalla, G. K., Faria, G. E., Silva, K. T., Castro, E. C., Reis, M. A., and Michelin, M. A. (2008) *Trypanosoma cruzi*: The role of PGE2 in immune response during the acute phase of experimental infection. *Exp. Parasitol.* **118,** 514–521
55. Schaller, J., and Gerber, S. S. (2011) The plasmin-antiplasmin system: Structural and functional aspects. *Cell. Mol. Life Sci.* **68,** 785–801
56. Franchini, M., and Lippi, G. (2010) Prothrombin complex concentrates: An update. *Blood Transfus.* **8,** 149–154
57. Jankun, J., Keck, R., Selman, S. H., and Skrzypczak-Jankun, E. (2010) Systemic or topical application of plasminogen activator inhibitor with extended half-life (VLHL PAI-1) reduces bleeding time and total blood loss. *Int. J. Mol. Med.* **26,** 501–504
58. Griffin, M. O., Jinno, M., Miles, L. A., and Villarreal, F. J. (2005) Reduction of myocardial infarct size by doxycycline: A role for plasmin inhibition. *Mol. Cell. Biochem.* **270,** 1–11
59. Aso, Y., Wakabayashi, S., Yamamoto, R., Matsutomo, R., Takebayashi, K., and Inukai, T. (2005) Metabolic syndrome accompanied by hypercholesterolemia is strongly associated with proinflammatory state and impairment of fibrinolysis in patients with type 2 diabetes: Synergistic effects of plasminogen activator inhibitor-1 and thrombin-activatable fibrinolysis inhibitor. *Diabetes Care* **28,** 2211–2216
60. Das, R., Pluskota, E., and Plow, E. F. (2010) Plasminogen and its receptors as regulators of cardiovascular inflammatory responses. *Trends Cardiovasc. Med.* **20,** 120–124
61. Sakkinen, P. A., Cushman, M., Psaty, B. M., Rodriguez, B., Boineau, R., Kuller, L. H., and Tracy, R. P. (1999) Relationship of plasmin generation to cardiovascular disease risk factors in elderly men and women. *Arterioscler. Thromb. Vasc. Biol.* **19,** 499–504
62. Herrera, R. N., Diaz, E., Perez Aguilar, R., Bianchi, J., Berman, S., and Luciardi, H. L. (2005) Prothrombotic state in early stages of chronic Chagas' disease: Its association with thrombotic risk factors. *Arch. Cardiol. Mex.* **75,** (Suppl. 3) S3–38–S3–48
63. Kim, J. H., Yu, Y. S., Min, B. H., and Kim, K. W. (2007) The role of clusterin in retinal development and free radical damage. *Br. J. Ophthalmol.* **91,** 1541–1546
64. Hineno, A., Kaneko, K., Yoshida, K., and Ikeda, S. I. (2011) Ceruloplasmin protects against rotenone-induced oxidative stress and neurotoxicity. *Neurochem. Res.* **36,** 2127–2135
65. Adamsson Eryd, S., Smith, J. G., Melander, O., Hedblad, B., and Engström, G. (2011) Inflammation-sensitive proteins and risk of atrial fibrillation: A population-based cohort study. *Eur. J. Epidemiol.* **26,** 449–455
66. Krishnan, N., Dickman, M. B., and Becker, D. F. (2008) Proline modulates the intracellular redox environment and protects mammalian cells against oxidative stress. *Free Radic. Biol. Med.* **44,** 671–681
67. Gutteridge, J. M. (1986) Antioxidant properties of the proteins caeruloplasmin, albumin and transferrin. A study of their activity in serum and synovial fluid from patients with rheumatoid arthritis. *Biochim. Biophys. Acta* **869,** 119–127
68. Cohen, M. P. (2003) Intervention strategies to prevent pathogenetic effects of glycated albumin. *Arch. Biochem. Biophys.* **419,** 25–30
69. Goldman, R. D., Khuon, S., Chou, Y. H., Opal, P., and Steinert, P. M. (1996) The function of intermediate filaments in cell shape and cytoskeletal integrity. *J. Cell Biol.* **134,** 971–983
70. Faé, K. C., Diefenbach da Silva, D., Bilate, A. M., Tanaka, A. C., Pomerantzeff, P. M., Kiss, M. H., Silva, C. A., Cunha-Neto, E., Kalil, J., and

Guilherme, L. (2008) PDIA3, HSPA5 and vimentin, proteins identified by 2-DE in the valvular tissue, are the target antigens of peripheral and heart infiltrating T cells from chronic rheumatic heart disease patients. *J. Autoimmun.* **31,** 136–141
71. Cunha-Neto, E., Dzau, V. J., Allen, P. D., Stamatiou, D., Benvenutti, L., Higuchi, M. L., Koyama, N. S., Silva, J. S., Kalil, J., and Liew, C. C. (2005) Cardiac gene expression profiling provides evidence for cytokinopathy as a molecular mechanism in Chagas' disease cardiomyopathy. *Am. J. Pathol.* **167,** 305–313
72. Richard, P., Charron, P., Carrier, L., Ledeuil, C., Cheav, T., Pichereau, C., Benaiche, A., Isnard, R., Dubourg, O., Burban, M., Gueffet, J. P., Millaire, A., Desnos, M., Schwartz, K., Hainque, B., and Komajda, M. (2003) Hypertrophic cardiomyopathy: Distribution of disease genes, spectrum of mutations, and implications for a molecular diagnosis strategy. *Circulation* **107,** 2227–2232
73. Poetter, K., Jiang, H., Hassanzadeh, S., Master, S. R., Chang, A., Dalakas, M. C., Rayment, I., Sellers, J. R., Fananapazir, L., and Epstein, N. D. (1996) Mutations in either the essential or regulatory light chains of myosin are associated with a rare myopathy in human heart and skeletal muscle. *Nat. Genet.* **13,** 63–69
74. Flavigny, J., Richard, P., Isnard, R., Carrier, L., Charron, P., Bonne, G., Forissier, J. F., Desnos, M., Dubourg, O., Komajda, M., Schwartz, K., and Hainque, B. (1998) Identification of two novel mutations in the ventricular regulatory myosin light chain gene (MYL2) associated with familial and classical forms of hypertrophic cardiomyopathy. *J. Mol. Med.* **76,** 208–214
75. Szczesna, D., Ghosh, D., Li, Q., Gomes, A. V., Guzman, G., Arana, C., Zhi, G., Stull, J. T., and Potter, J. D. (2001) Familial hypertrophic cardiomyopathy mutations in the regulatory light chains of myosin affect their structure, Ca^{2+} binding, and phosphorylation. *J. Biol. Chem.* **276,** 7086–7092
76. Pannu, H., Tran-Fadulu, V., Papke, C. L., Scherer, S., Liu, Y., Presley, C., Guo, D., Estrera, A. L., Safi, H. J., Brasier, A. R., Vick, G. W., Marian, A. J., Raman, C. S., Buja, L. M., and Milewicz, D. M. (2007) MYH11 mutations result in a distinct vascular pathology driven by insulin-like growth factor 1 and angiotensin II. *Hum. Mol. Genet.* **16,** 2453–2462
77. Pannu, H., Avidan, N., Tran-Fadulu, V., and Milewicz, D. M. (2006) Genetic basis of thoracic aortic aneurysms and dissections: Potential relevance to abdominal aortic aneurysms. *Ann. N.Y. Acad. Sci.* **1085,** 242–255
78. Milewicz, D. M., Guo, D. C., Tran-Fadulu, V., Lafont, A. L., Papke, C. L., Inamoto, S., Kwartler, C. S., and Pannu, H. (2008) Genetic basis of thoracic aortic aneurysms and dissections: Focus on smooth muscle cell contractile dysfunction. *Annu. Rev. Genomics Hum. Genet.* **9,** 283–302
79. Janssen, M. E., Kim, E., Liu, H., Fujimoto, L. M., Bobkov, A., Volkmann, N., and Hanein, D. (2006) Three-dimensional structure of vinculin bound to actin filaments. *Mol. Cell* **21,** 271–281
80. Zemljic-Harpf, A., Manso, A. M., and Ross, R. S. (2009) Vinculin and talin: Focus on the myocardium. *J. Investig. Med.* **57,** 849–855
81. Dhiman, M., and Garg, N. J. (2011) NADPH oxidase inhibition ameliorates Trypanosoma cruzi-induced myocarditis during Chagas disease. *J. Pathol.* **225,** 583–596.